Colloidal Plasmonic Nanocomposites: From Fabrication to Optical Function

Su-Wen Hsu, Andrea L. Rodarte, Gaurav Arya, Madhura Som, and Andrea R. Tao*

Department of NanoEngineering, University of California, San Diego, 9500 Gilman Dr. MC 0448, La Jolla, California 92039-0448, United States

*Email: atao@eng.ucsd.edu

TOC Figure:

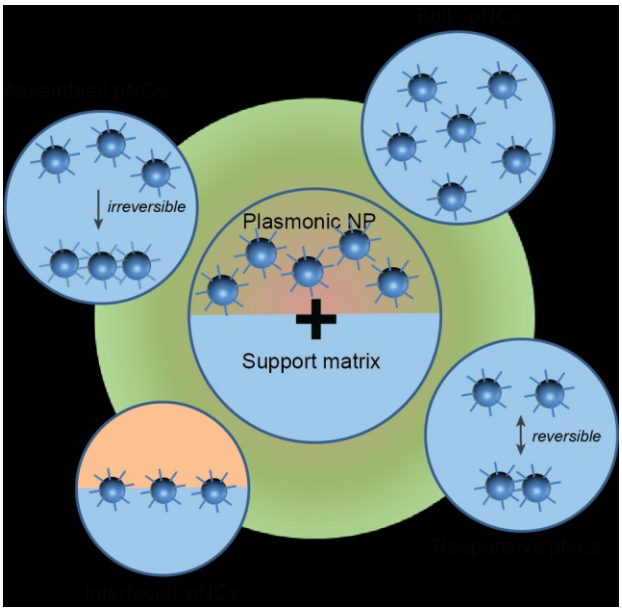

Abstract:

Plasmonic nanostructures are extensively used building blocks for engineering optical materials

and device architectures. Plasmonic nanocomposites (pNCs) are an emerging class of materials that integrate these nanostructures into hierarchical and often multifunctional systems. These pNCs can be highly customizable by modifying both the plasmonic and matrix components, as well as by controlling the nano- to macroscale morphology of the composite as a whole. Assembly at the nanoscale plays a particularly important role in the design of pNCs that exhibit complex or responsive optical function. Due to their scalability and tunability, pNCs provide a versatile platform for engineering new plasmonic materials and for facile integration into optoelectronic device architectures. This review provides a comprehensive survey of recent achievements in pNC structure, design, fabrication, and optical function along with some examples of their application in optoelectronics and sensing.

Table of Contents

1. Introduction

Plasmonic nanocomposites (pNCs) are emerging materials that have the potential to transform a variety of applications where light management is critical, such as local refractive index sensing, light trapping in photovoltaic devices, label-free analyte detection, and nanoscale optics. A simple description of a pNC consists of a plasmonic component, typically a metal particle or nanostructure, encapsulated within a dielectric matrix such as polymer or glass. One of the oldest known pNCs can be found in the 1,600-year-old Roman chalice known as the Lycurgus Cup, where 70 nm silver and gold particles are isotropically embedded within glass. These nanoparticles, which support surface plasmon resonances in the visible range, provide the glass cup with its characteristic dichroic quality, where it appears jade-green when illuminated from outside the chalice and wine-red when illuminated from inside. The Lycurgus Cup is an excellent example the glass and ceramic plasmonic composites that have been utilized by artisans for more than centuries for their unique color profiles. (Figure 1) Today, pNCs provide access to an entirely new set of materials functions, including optical confinement and enhanced spectroscopy. Recent advances in the synthesis, assembly, and characterization of nanomaterials are now enabling a new generation of pNCs whose structures are highly engineered to elicit a specific far-field or near-field optical response. The ability to design these functional nanocomposites with precision is critical for the integration of plasmonic components into device platforms and architectures. The motivation of this review is to provide an overview of pNC fabrication, processing, and device integration, as well as to provide an outlook on state-of-the-art plasmonic nanomaterials.

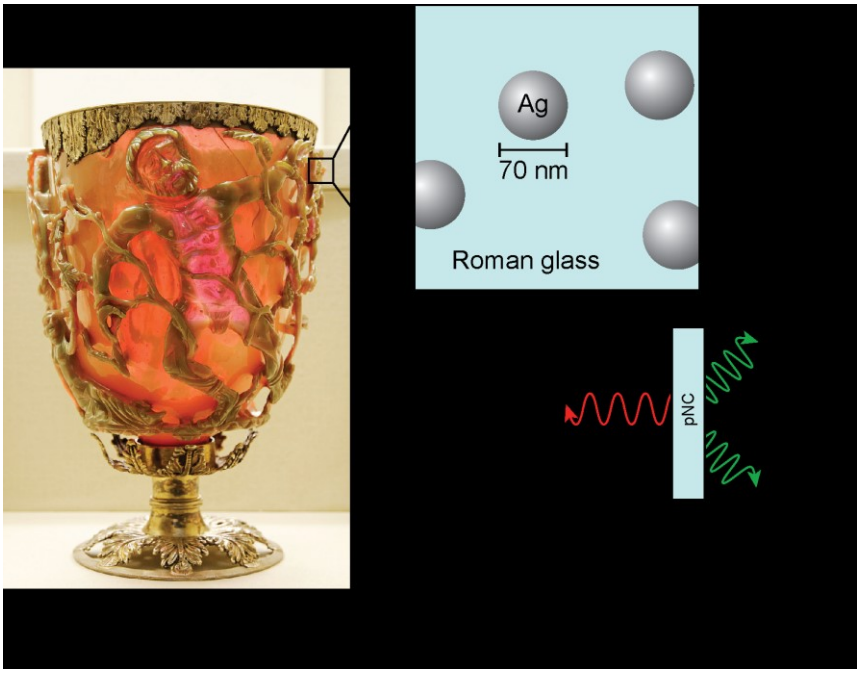

Figure 1. The Lycurgus Cup, one of the oldest known plasmonic nanocomposites, is composed of Roman glass embedded with 70 nm Ag-Au alloyed nanoparticles and can be classified as a bulk pNC. The extinction spectrum of a colloidal dispersion of similarly sized Ag nanoparticles shows the strong scattering response due to plasmonic excitation at green wavelengths. As a result, the thick regions of the cup where scattering processes are dominant appear olive green, whereas thinner regions where transmission is dominant appear red. Photo by Marie-Lan Nguyen is licensed under CC BY 2.5.

1.1 Background

pNCs are heterogeneous, multicomponent systems. At the basic constituent level, they can also be classified as metal-insulator composites, where nanoscale metallic particles or inclusions are dispersed within or on a dielectric substrate. However, early on researchers realized that the behavior of pNCs did not adhere to simple scaling laws (e.g. a “rule of mixtures”) that are used to characterize traditional composite materials. The optical properties of these materials fail to scale with particle volume fraction. In the mid-1980s,[1] researchers observed that metal-insulator composites consisting of isotropically distributed Au nanoparticles exhibited anomalously high absorbance values near the percolation threshold, where the particles approached long-range

connectivity. This absorption could not be accounted for by effective medium theories such as Maxwell-Garnett and Bruggemann approaches, which only explained optical behavior at very low or very high particle volume fractions. These early studies highlighted the importance of the local arrangement of the metal constituents, which we now know plays a critical role in determining the optical behavior of these composite materials.

Today, we recognize that these anomalous optical properties arise from the excitation of surface plasmons. Surface plasmons are coherent electron oscillations that are driven at the frequency of the incident electromagnetic field. These charge oscillations result in intense and highly localized electromagnetic fields that are trapped near the metal surface and can be confined to volumes that are smaller than the diffraction limit. Propagating surface plasmons are excited at metal-dielectric interfaces and result in near-fields that are strongly localized in one-dimension. Localized surface plasmon resonances (LSPRs) are supported by metal nanoparticles and nanostructures that are smaller than the wavelength of light. When excited, LSPRs cause the incident electromagnetic field to become strongly localized to the surface of the particle.

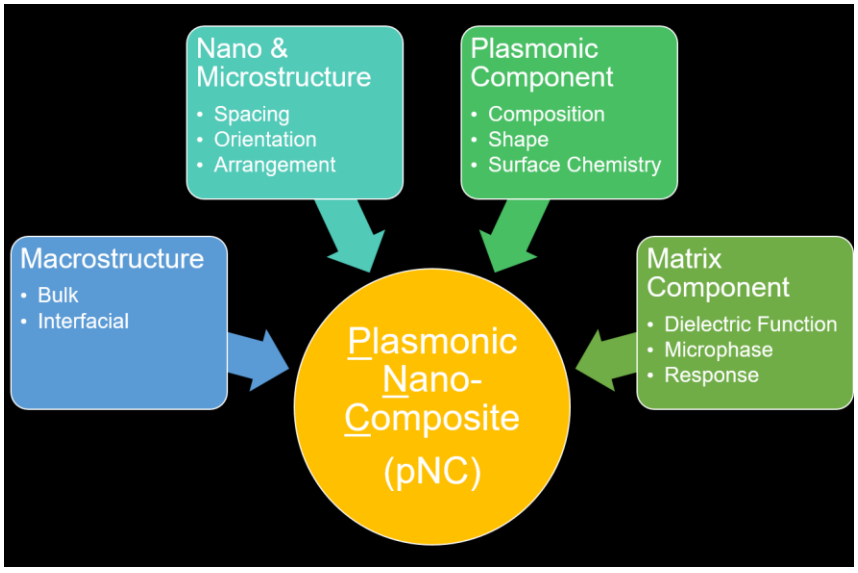

Figure 2. Parameters that affect the electromagnetic response of pNCs.

Metallic Ag and Au nanoparticles are the most widely utilized building blocks of pNCs. These metals possess dielectric functions with a negative real component and small positive imaginary component, enabling surface plasmon excitation in the visible spectrum. (Semimetals and doped semiconductors also support plasmon excitation, but possess lower free carrier concentrations such that excitation occurs in the near- to- mid-infrared range.) Nanoparticle size and shape are also critical determinants of LSPR wavelength and near-field intensities, since the excited charge wave is essentially bound to the particle geometry. For example, nanoparticles with anisotropic shapes exhibit high field localization at sharp corners, which is advantageous for application in surface-enhanced Raman scattering and fluorescence enhancement. Ag and Au nanoparticles can also exhibit large scattering and/or absorbance cross-sections at the resonance wavelength, which is the basis for refractive index sensing and plasmonic structural colors.

Plasmonic coupling is observed when two metal interfaces (either from nanoparticles or thin-films) are brought into close proximity. The strength of this capacitive coupling across the dielectric gap is highly dependent on gap distance. Weak coupling is observed at gap distances larger than 20 nm. Strong coupling is typically observed for gap distances <20 nm, and can result in energy transfer between neighboring particles, large shifts in the resonant frequency, and extreme light confinement. For example, nanojunctions between two Ag nanoparticles or an Ag nanoparticle and Au thin-film can be designed to generate electromagnetic hot spots where the resulting near-field is several orders of magnitude stronger than the incident field.[2-3] For shaped nanoparticles, interparticle orientation is also a critical factor in determining coupling strength. Gap distances < 1 nm have been observed to exhibit quantum effects such as electron tunneling. Due to these varying coupling regimes, the optical behavior of pNCs is highly dependent on plasmonic component spacing and arrangement within the dielectric matrix.

1.2 Classification of Plasmonic Nanocomposites

In this review, we primarily focus on pNCs that consist of metal nanoparticle building blocks introduced into a dielectric medium or interface. Plasmonic metamaterials and metasurfaces generated by photolithography or layer-by-layer deposition are also an important category of pNCs, but their fabrication and characterization have been described extensively elsewhere in the literature.[4-5] For ease of discussion, we categorize pNCs into the following four main categories that are primarily determined by pNC architecture (Figure 3):

- Isotropic or bulk pNCs: Plasmonic components are distributed isotropically within a dielectric matrix. Here, we define bulk pNCs as composites that can be described by effective medium theories, with the plasmonic nanocomponents typically comprising a low volume fraction of the total material. In most cases, the dielectric matrix serves as an insulating barrier between plasmonic components, but can also contribute to optical or electronic function. Nanoparticles can be isotropically distributed while adopting specific orientations within the matrix.
- Assembled pNCs: Plasmonic components are organized into clusters or regions of anisotropic density within a dielectric matrix. The directed or self-assembly of particles is typically desired for the formation of nanojunctions, where strong plasmonic coupling is present. The pNC possesses behavior characterized by the collective optical properties of the plasmonic components. Nanoparticle assembly is often carried out within a fluid or viscoelastic matrix.
- Responsive pNCs: Plasmonic components can be rearranged to exhibit a tunable or adaptive electromagnetic response. These composites are typically a subset of assembled pNCs, but are categorized separately due to their unique function.
- Interfacial pNCs: Plasmonic nanoparticles that straddle a metal-dielectric or dielectric-dielectric interface. These composites are often two-dimensional (2D) and engineered

for integration within planar device architectures. The plasmonic component of the composite possesses optical or electronic properties that are distinct from bulk or assembled pNCs.

The remainder of the review discusses each of these pNC categories in detail, from fabrication and processing to characterization of pNC properties.

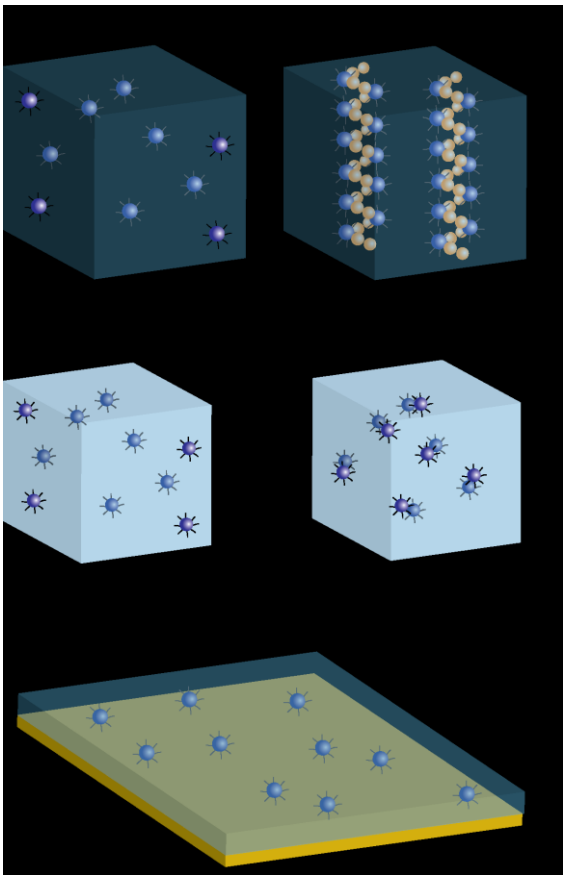

Figure 3. Schematic of the various classes of pNCs described in this review.

2. Bulk pNCs

2.1 Nanoparticles in Solids

Solid pNCs are typically comprised of bulk nanocomposites where metal nanoparticles are incorporated into glass and ceramic materials. Glasses composed of SiO_2 and TiO_2 offer

several advantages as a matrix for plasmonic components, including high transparency in the ultraviolet and visible range, good mechanical strength, and amorphous materials structure that readily accommodates nanoparticle encapsulation. Given the long-history of metal nanoparticle incorporation into oxide matrices[6-9], here we focus only on the most recent advances in this category of pNCs. Previously, the fabrication methods for solid pNCs required approaches that necessitate high temperature treatments or high energy irradiation due to the high melting temperature of common glasses.[10] Recent work has made progress in the development of simple encapsulation methods for solid pNC fabrication, which have been demonstrated for enhanced photocatalysis and photoluminescence. Fang et al. fabricated mesoporous Au-TiO_2 pNCs using a sol-gel method, where a poly(ethylene glycol)-based co-polymer enables chemical compatibility with silica systems and 99.9% transmittance in the ultraviolet and visible range. The co-polymer forms micelles that serve as a sacrificial skeleton for silica coating, and is then burned out to create a porous template for metal nanoparticle generation. These pNCs were observed to be excellent materials for light-driven H_2 evolution, which is attributed to plasmon-assisted hot electron generation by the Au nanoparticle and subsequent electron transfer to the TiO_2.[11] Som et al. developed a single-step melt-quench method to synthesize plasmonic Au and Ag NPs embedded in both glass and ceramic matrices, where a molten Sb_2O_3-based matrix acts as a mild reducing agent for metal salts. The high viscosity Sb_2O_3 matrix also plays a critical role in templating the nucleation and growth of anisotropic nanoparticles with different sizes and shapes. The pNCs are made by melting the mixture of metal and glass precursors, casting the molten mixture into a carbon plate for annealing, and finally slowly cooling down to room temperature to partially crystallization the Sb_2O_3 matrix.[12-15]

In applications where the desired outcome is enhanced photoabsorption or emission, the plasmonic component is often separated by a thin dielectric barrier to prevent quenching. Core-shell structures where Ag nanoparticles are encapsulated by a thin SiO_2 shell are often the basis for upconverting pNCs, where the core-shells are co-embedded with rare earth ions such

as Sm^{3+} and Er^{3+} into a dielectric matrix. The SiO_2 shell serves as a tunable spacer to control the distance between the Ag core and upconversion material.[16-17] More recent work has incorporated similar plasmonic core-shells into perovskite layers for enhanced photovoltaic performance by enhancing topical absorption[18-19] and increasing hole transport.[20] Zhang et al. incorporated SiO_2–encapsulated Au nanoparticles into organometal halide perovskite solar cells, resulting in an average efficiency increase from 8.4% to 9.5%.[21] They showed that this increased efficiency was not due to enhanced light absorption, but instead resulted from reduced exciton binding energy and enhanced generation of free-charge carriers in the active layer.

2.2 Nanoparticles in Polymers

Polymer pNCs possess unique mechanical behavior (stiffness, flexibility, Young's modulus) and physical properties (glass transition, viscosity) properties that distinguish them from their solid-state counterparts. Polymers also serve as a convenient dielectric matrix that is amenable to solution-based and scalable processing. The fabrication of bulk polymer pNCs can be classified into two broad groups: (1) *in situ* methods where plasmonic nanoparticle components are synthesized directly within a polymer matrix, and (2) nanoparticle-polymer blends where preformed plasmonic nanoparticles are mixed to form a binary or multiphasic mixture. These techniques have been well-developed for the fabrication of generic particle-polymer composites and have been translated for the preparation of pNCs. In the following sections, we review the most widely employed fabrication methods and architectures of polymer pNCs.

2.2.1 *In situ* synthesis

In situ synthesis typically involves the reduction of Ag or Au salts that are pre-loaded into the matrix polymer. Metal salt reduction can be achieved by thermolysis,[22-24] irradiation with a high energy source (e.g. electron beam, ion beam, or X-ray),[25-27] or chemical reduction using agents

such as $NaBH_4$, H_2, hydrazine, or reaction with the polymer matrix itself.[28-35] One example of the latter are pNCs composed of polyvinyl acetate (PVA), poly(methyl methacrylate) (PMMA), and poly *N*-acylethylenimine, all of which can serve as reducing agents for Ag^{I} and Au^{III}.[35] In general, the size and shape of metal NPs generated within a polymer matrix can be controlled by adjusting the reducing power (e.g. temperature or irradiation dose rate). The polymer matrix also plays a critical role in dictating the properties of the resulting pNC by serving as a template for metal nanoparticle nucleation and growth. Specific examples of this are outlined below:

- Hydrogels: The three-dimensional polymer network characteristic of hydrogels serves as a suitable template for nanoparticle growth. Nanoparticle size and clustering is typically controlled by crosslinking density of the hydrogel network, where free space in the swollen hydrogel serve as "nanoreactors" for nanoparticle growth (Figure 4b).[32] Hydrogels can also be designed to possess chemical moieties that anchor metal salts,[36] as demonstrated by the metal-chitosan pNCs fabricated by Huang et al.[37]
- Photoresist: In these pNCs, optical or electron-beam lithography can be used to simultaneously pattern the polymer matrix and nucleate metal nanoparticles. The plasmon response of the resulting pNCs can be tuned through the metal salt loading concentration and post-bake conditions, both of which alter nanoparticle size and shape (Figure 4c).[22] Electron-beam writing can also be carried out to direct-write plasmonic components within these pNCs. Abargues et al. demonstrated that for Ag^{I} loaded inside a PVA-based negative resist, electron beam irradiation is sufficient to both cross-link PVA and form dense regions of Ag nanoparticles.[26]
- Block co-Polymers (BCPs): Carrying out metal salt reduction within the ordered polymer domains of BCPs is one strategy for generating dense and highly ordered plasmonic nanoparticle arrays over large areas. Metal salts and complexes can be readily loaded into the lamella or micelles formed by hydrophilic BCP domains, and the ordered BCP morphology is typically retained for the formation of nanoparticles between 2-12.5 nm in

diameter.[30] In this manner, pNCs that possess long-range hexagonal order[28] or periodic lamellar morphologies (Figure 4D).[29] This is advantageous for the generation of bulk pNCs that possess an isotropic optical response. Control over the optical response of the resulting pNCs can be improved by crosslinking the BCP and selective swelling of BCP domains.[38]

In-situ pNC synthesis can also be carried out by using techniques that involve simultaneous nanoparticle growth and polymerization. Microwave-assisted pNC synthesis has been used to fabricate a homogeneous distribution of metal nanoparticles within an acrylamide medium[39-40] and ultraviolet irradiation has been similarly employed for pNCs with an acrylonitrile matrix.[41] A significant advantage of these irradiation methods is that no additional reducing agent or polymerization initiator is required; plasmon response can be tuned through irradiation power alone. Physical deposition methods such as co-evaporation or co-sputtering also do not require chemical reduction for pNC formation. In these methods, tunable optical response is controlled by metal fill factor, cluster size, and interparticle separation distance. Metal fill factor has been demonstrated for an extremely wide range, between 4-80% by co-sputtering.[42] These methods allow for the quick deposition of mechanically and chemically robust dielectric media, such as polytetrafluoroethylene (PTFE), which would otherwise be difficult to fabricate as composites. For example, Schürmann et al. formed Ag nanoparticles distributed isotropically within a PTFE matrix by co-sputtering Ag and PTFE, using the direct current sputtering power as a knob for tuning the LSPR of the Ag nanoparticles in the visible range.[43-44] Physical deposition methods also allow for flexibility in the choice of metal target. This can be useful for generating plasmonic nanoparticles from exotic metals or from metal alloys, where independent metal deposition rates can be used to dictate the final nanoparticle composition.[45]

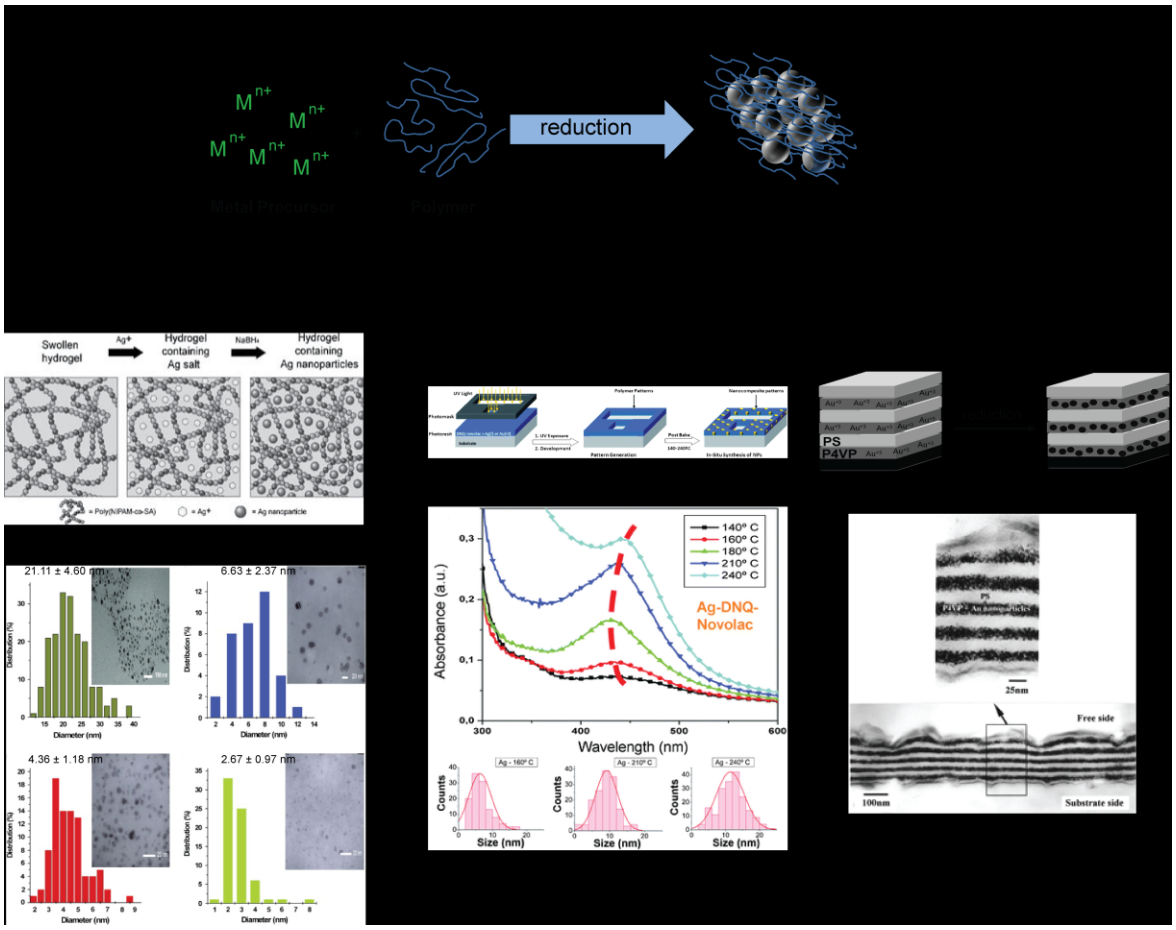

Figure 4. a) In situ synthesis of polymer-nanoparticle pNCs. Metal salt precursor is dispersed in the polymer matrix followed by reduction. b) Three-dimensional polymer network of the hydrogel, poly[N-isopropylacrylamide-co-(sodium acrylate)], acts as the template for the synthesis of well-dispersed metal nanoparticles. The size of nanoparticles can be tuned from 21.11 ± 4.60, 6.63 ± 2.37, 4.36 ± 1.18, to 2.67 ± 0.97 nm by controlling the degree of cross-linking of hydrogel.[32,36] Reproduced with permission from ref 32. Copyright 2007 Elsevier, Ltd. and Reproduced with permission from ref 36. Copyright 2006 Wiley Periodicals, Inc. c) Photosensitive polymer can be used to fabricate nanocomposite patterns. The average size of NPs change from 6.3 ± 3.3 nm to 11.4 ± 4.1 nm by increasing baked temp. from 160 to 240°C, causing the LSPR peak of the pNC to red-shift from 433 to 449 nm.[22] Reproduced with permission from ref 22. Copyright 2010 The Royal Society of Chemistry. d) The lamellae structure of polystyrene-block-poly(4-vinylpyridine), PS-b-P4VP, is used as a template for selective synthesis of Au nanoparticles in the P4VP domain. Au precursor coordinates to the pyridine units of P4VP, templating nanoparticle

nucleation as shown in cross-sectional TEM images.[29] Reproduced with permission from ref 29. Copyright 2001 American Chemical Society.

2.2.2 Nanoparticle-Polymer Blends

A major disadvantage of in situ synthesis methods for producing pNCs is that these techniques tend to produce plasmonic nanoparticles that are largely polydisperse in both morphology and particle size. The fabrication of plasmonic nanoparticle-polymer blends overcomes this challenge by incorporating already synthesized metal nanoparticles into a polymer matrix. Because each component of the pNC is synthesized independently, pNCs can be fabricated in a combinatorial manner with the potential to generate a wide range of multifunctional nanocomposites. For pNCs, a significant advantage is the incorporation of shaped metal nanoparticle building blocks that possess tailored LSPRs.[46-53] Shaped pNCs — such as nanorods, nanocubes, and triangular nanoprisms — possess higher order LSPRs and large electromagnetic field enhancements due to the presence of sharp corners and edges.

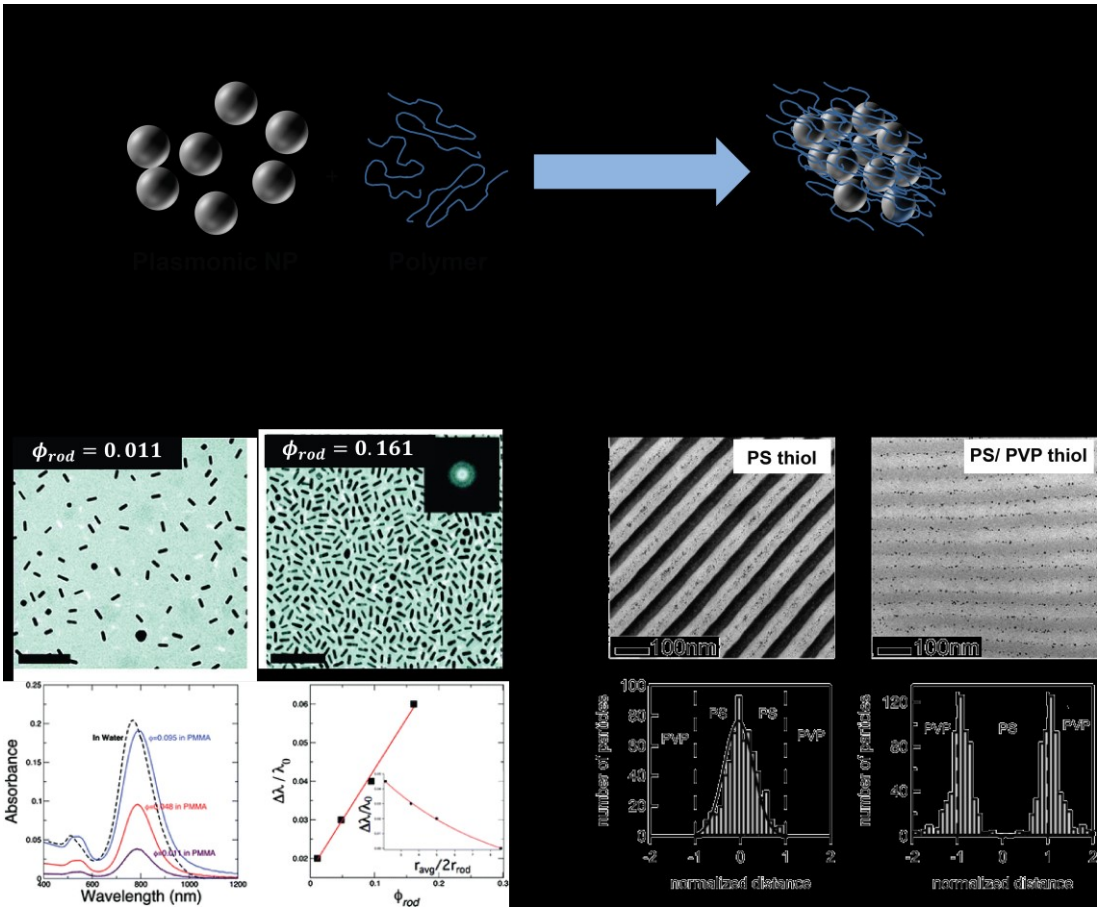

Figure 5. a) Schematic of nanoparticle-polymer blends for pNC fabrication. b) Poly(ethylene glycol) (PEG)-functionalized Au nanorods self-assemble in a poly(methyl methacrylate) (PMMA) film. The average spacing between nanorods and absorption of the nanocomposite can be tuned by changing the volume fraction of Au NRs (ϕ_{rod}). As ϕ_{rod} increasing from 1 to 16 vol %, the average spacing between NRs decreases from 120 to 20 nm and causes the a red-shift of the LSPR peak.[54] Reproduced with permission from ref 54. Copyright 2010 American Chemical Society.c) The location of nanoparticles in a BCP matrix can be adjusted by tuning miscibility of the particles and BCP domains.[55] Reproduced with permission from ref 55. Copyright 2005 American Chemical Society.

Chemical modification of the nanoparticle surface is critical in the fabrication of blended pNCs. To prevent unwanted agglomeration or phase separation, plasmonic components are typically grafted with polymer chains that are miscible with the polymer matrix. Grafts with large radii of gyration and/or grafts tethered at a high surface density impart the maximum possible

stability to the polymer blend.[56] For example, Au nanorods grafted with polystyrene [57] and embedded in a PS thin-film show a strong optical resonance at 780 nm consistent with excitation of the longitudinal dipolar LSPR mode. For long grafts and short matrix polymer, the Au nanorods remain effectively dispersed and optically isolated within the pNC. For longer matrix polymer chains, the optical response of the pNC shows a clear blue-shift of the LSPR resonance due to the formation of nanorod aggregates.[58] Selection of appropriate polymer grafts is crucial for achieving isotropic nanoparticle distribution, even at high loading densities. For example, by selecting a polyethylene glycol (PEG) graft for Au nanorods, the nanorod loading into a poly(methyl methacrylate) (PMMA) matrix could be increased up to a 16% volume fraction while still remaining uniformly dispersed. As a result, the average spacing between nanorods decreases from 120 nm to 20 nm, causing the LSPR peak to red-shift about 50 nm due to weak plasmon coupling.[54] (Figure 5b)

Polymer grafts not only prevent agglomeration, but also play an integral role in tuning the electromagnetic response of the pNC through the control of interparticle spacing. In the strong-coupling regime, field localization can result in extreme optical confinement, highly polarized near-fields, and large wavelength shifts in the far-field optical response. Appropriate selection of polymer graft length can dictate whether or not the pNC exhibits these electromagnetic coupling effects. Polymers grafted on the nanoparticle surface can be used as molecular spacers to control particle separation distances, where the degree of plasmonic coupling is determined by the length of the grafted chain. (Figure 6) Moreover, the grafts provide an entropic barrier to touching or fused nanoparticles. For example, spherical Au nanoparticles form clusters after surface modification with poly(oxypropylene)diamines. The bifunctional polymer serves to cross-link particles, and as molecular weight of the polymer increases from 230 to 4000 g mol^{-1}, interparticle distances increase from 2.7 $\pm$ 0.7 nm to 7.3 $\pm$ 1.3 nm. Correspondingly, the LSPR wavelength of these aggregates shows a large blue-shift from 759 nm to 569 nm.[59] (*Figure 6*a) Dendritic polymers can also serve as effective spacer molecules that accurately govern

interparticle spacing with sub-nanometer accuracy.[60] (*Figure 6*b)

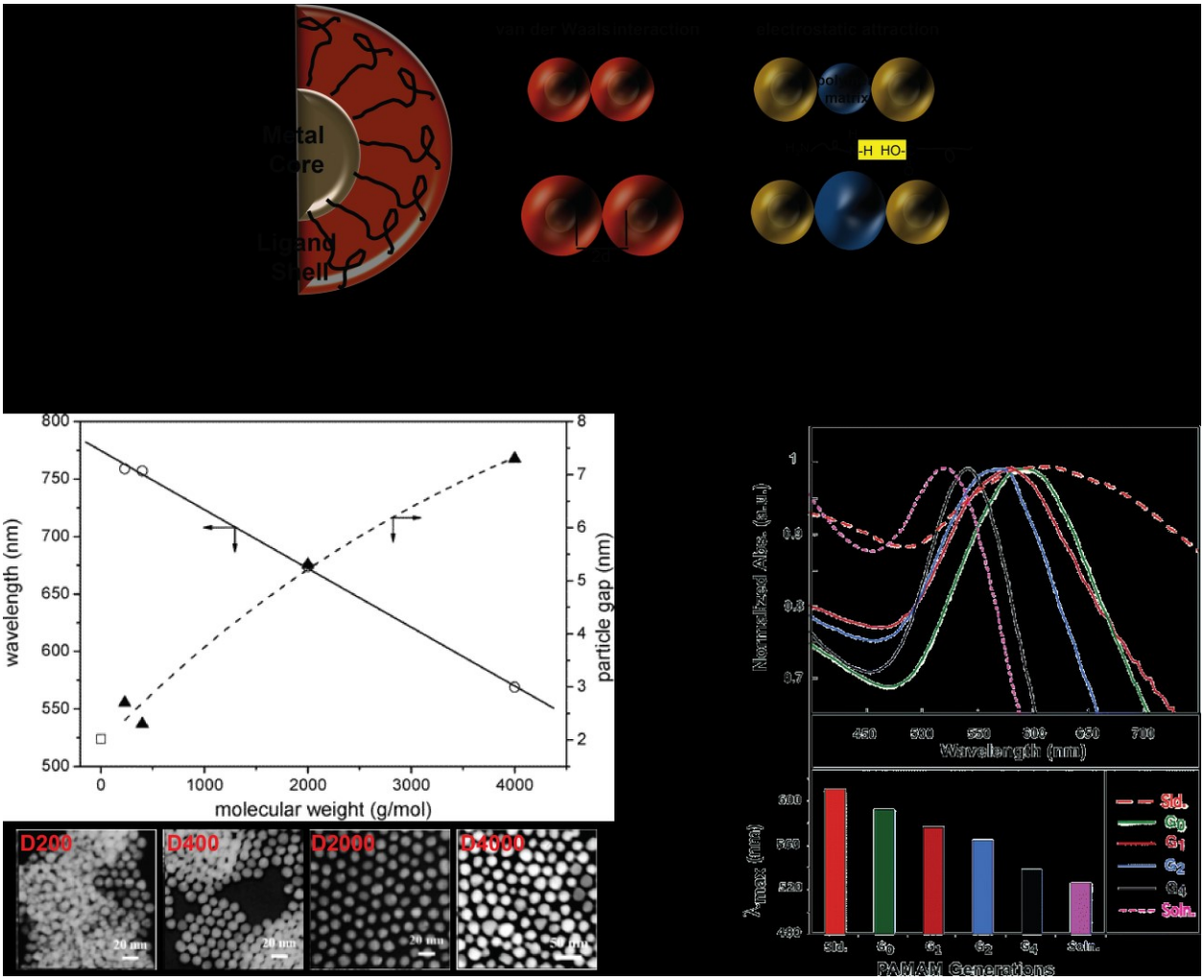

Figure 6. Schematic of two strategies to control the spacing between nanoparticles in a homopolymer matrix. a) Au nanoparticles are functionalized with poly(oxypropylene)diamines, then self-assembled into 2D and 3D nanocomposites with tunable spacing by controlling the molecular weight of the polymer chain.[59] Reproduced with permission from ref 59. Copyright 2005 American Chemical Society. *b) Dendritic ligands, such as poly(amidoamine), act as molecular spacer to accurately control interparticle spacing. Equilibrium particle distance is maintained by the electrostatic attraction between the amine-terminated polymer matrix and the carboxylic acid- terminated the Au nanoparticles.*[60] Reproduced with permission from ref 60. Copyright 2005 American Chemical Society.

In many cases, such as the fabrication of metamaterials and plasmonic arrays, pNCs with periodic morphologies are desired. The use of BCPs in blended pNCs has been somewhat successful in creating pNCs with more sophisticated control of nanoparticle distribution. Similar to pNCs generated by in situ nanoparticle synthesis in BCP templates, blended pNCs take advantage of the various BCP phases to control nanoparticle distribution. Plasmonic nanoparticles can be modified to either reside in a particular BCP domain, or to reside at the interface between two domains by controlling the surface chemistry of the NPs. For example, Au nanoparticles with sizes of 3.9 $\pm$ 1.0 nm can be integrated into a matrix of poly(styrene-b-2 vinyl pyridine) (PS-PVP). When the nanoparticle is modified by either PS-thiol, PVP-thiol, or a mixture of PS-thiol/ PVP thiol, the nanoparticles migrate to either the PS domain, PVP domain, or the interface between the PS and PVP domain, respectively.[55,61-62](Figure 5c) In this manner, plasmonic nanoparticles can be loaded into BCP matrices at high loading fractions (up to 0.5) without macrophase segregation.[63] A significant disadvantage of these BCP templates, however, is that at least one of the BCP microdomain dimensions must be near equal to or significantly larger than the nanoparticle dimensions in order to avoid significant distortion of the BCP microphase structure. Few BCP-based pNCs have been generated with nanoparticles >30 nm, which is typically the size of metal nanoparticle employed for LSPR excitation.

For the generation of pNCs, more sophisticated control over the nano- and mesoscale morphology of metal-polymer nanocomposites is necessary. In general, the above methods have been optimized mainly for spherical NPs or low aspect-ratio nanorods as the plasmonic component. However, many novel optical effects derived from plasmon excitation require components that possess higher shape anisotropy (e.g. antenna effects) or large aspect-ratios (e.g. plasmonic waveguiding). *In situ* methods are also limited in the integration of plasmonic components with already existing electronic or optical components. The ability to control NP spacing is limited when synthesizing NPs that possess large size distributions and poor dispersity. These challenges with bulk polymer pNC fabrication point towards self- or directed

assembly techniques as more viable options for generating composites with advanced plasmonic function.

3. Assembled pNCs

In recent years, intense focus has been directed toward plasmonic materials that exhibit advanced optical functions by rationally engineering how plasmonic nanostructures self-assemble and perform within complex nanocomposite materials. This opportunity stems from the convergence of two major developments and discoveries. First is the realization that solid-state nanoparticles functionalized with polymers can be assembled into a rich variety of architectures. Specifically, the ability to synthesize nanoparticles with anisotropic shapes has provided a new arena of phase space for state-of-the-art nanocomposites. Second is the burgeoning field of optical metamaterials and metasurfaces, where researchers have predicted and experimentally demonstrated that plasmonic nanocomponents can be arranged into mesostructured materials architectures that give rise to novel optical phenomena such as negative index of refraction, fast and slow light propagation, and perfect lensing. The challenges in fabricating these hierarchical structures using top-down fabrication techniques has spurred interest in bottom-up approaches such as self-assembly to overcome obstacles in nanomanufacturing that include scalability, designing flat and precise metal surfaces, and engineering three-dimensional mesostructures.

Self- and directed assembly provides a bottom-up approach to the fabrication of pNCs and has been demonstrated to achieve precise nanoparticle arrangements in a massively parallel, scalable manner. Polymer-based pNCs are especially attractive as they allow for facile device integration using techniques that take advantage of batch, low-cost processing. In the sections below, we outline three major types of pNC architectures generated by assembly

methods, present strategies for fabrication, and provide a general framework for understanding the optical response of each type.

3.1 Periodic pNCs

Periodic arrangements or arrays of plasmonic nanostructures are highly desired structures for a wide range of optical applications, including metamaterials[64-67] and ultrasensitive spectroscopic sensing.[68-70] For example, ordered two-dimensional (2D) arrays of metal nanoparticles can give rise to sharp Fano resonances that can be utilized in LSPR sensing for chemical binding events.[71-74] The templated assembly of nanoparticles within a pNC offers a scalable route for fabricating such ordered structures. One strategy for generating a periodic pNC is by ordering plasmonic nanoparticles within self-ordering soft materials such as BCPs and liquid crystals. Nanoparticles introduced into BCPs can be directed to co-assemble into periodic 1-, 2-, and 3-dimensional arrays by engineering nanoparticle surface chemistries to interact selectively with the microdomains of a given BCP. For example, Kao et al. demonstrated that Au nanoparticles assemble into 1D periodic chains when integrated into the lamellar structure of a supramolecular BCP that contains a PS block. When a similar BCP architecture is modified to adopt a cylindrical phase, the Au nanoparticles are excluded from the cylindrical PS cores and form periodic 2D hexagonal arrays in the interstitial sites of the cylindrical domains.[75-76] This assembly strategy can be extended to anisotropic plasmonic building blocks, such as Au nanorods, where nanorod confinement within the BCP framework results in end-to-end oriented 1D arrays for moderate nanorod loading densities (3−6 vol %).[77] Additional control over BCP-base pNCs can be obtained by utilizing additional hard templates or surface patterning to direct co-assembly.[78] (Figure 7a) Shukla et al. obtained 2D Au nanorod arrays that support coupled transverse LSPR modes in the near-infrared by co-polymerizing nanorods and polymer within porous alumina templates.[79]

Anisotropic plasmonic components such as Au nanorods present particularly interesting

building blocks for periodic pNCs, since their optical response is highly dependent on interparticle orientation within the pNC. Ng et al. fabricated free-standing 2D superlattices of PS-grafted Au nanorods with two types of arrangements: horizontally-aligned and vertically-aligned nanorods. The nanorods form self-assembled sheets in these two orientations, where solvent evaporation rate is the primary determinant for sheet orientation. As a result, the optical extinction of the periodic pNC is highly polarized along the axis of alignment rather than the nanorod axes due to strong coupling between neighboring nanorods.[80] For example, coupling between the longitudinal LSPRs of the nanorods results in a polarized field perpendicular to the nanorods' long axes. More exotic periodic pNCs structures can be constructed by explicitly controlling nanorod orientation within a soft matrix. For example, chiral pNCs were obtained from incorporating Au nanorods into a macroscopic cholesteric film formed by self-assembled cellulose nanocrystals. In this system, the cholesteric host dictates pNC periodicity and order, leading to a pNC that exhibits strong circular dichroism and polarization rotator function. Similar to other superlattice structures, the strength of plasmonic chiroptical activity exhibited by the pNC strongly depends on the dipole-dipole interactions and interparticle spacing of coupled Au nanorods.[81-82] (Figure 7b)

Overall, the morphology of nanostructured matrices such as BCPs or cholesteric films serves as a director for the resulting pNC morphology. As a result, pNC parameters such as NP orientation and cluster size are highly limited by the domain geometries of the matrix. As such, it may be difficult to use these templating strategies to assemble NPs into plasmonic junctions or tightly-spaced cluster. For example, the spacing between NPs can be reduced to sub-10 nm by choosing a BCP that possesses a narrow domain size or by increasing NP loading prior to pNC phase segregation. However, achieving strong electronic-plasmonic or photon-plasmonic coupling typically requires interparticle spacings in the range of 1-3 nm. This small spacing is difficult to achieve by BCPs due to the instability of periodic BCP phases with high NP loading

density.

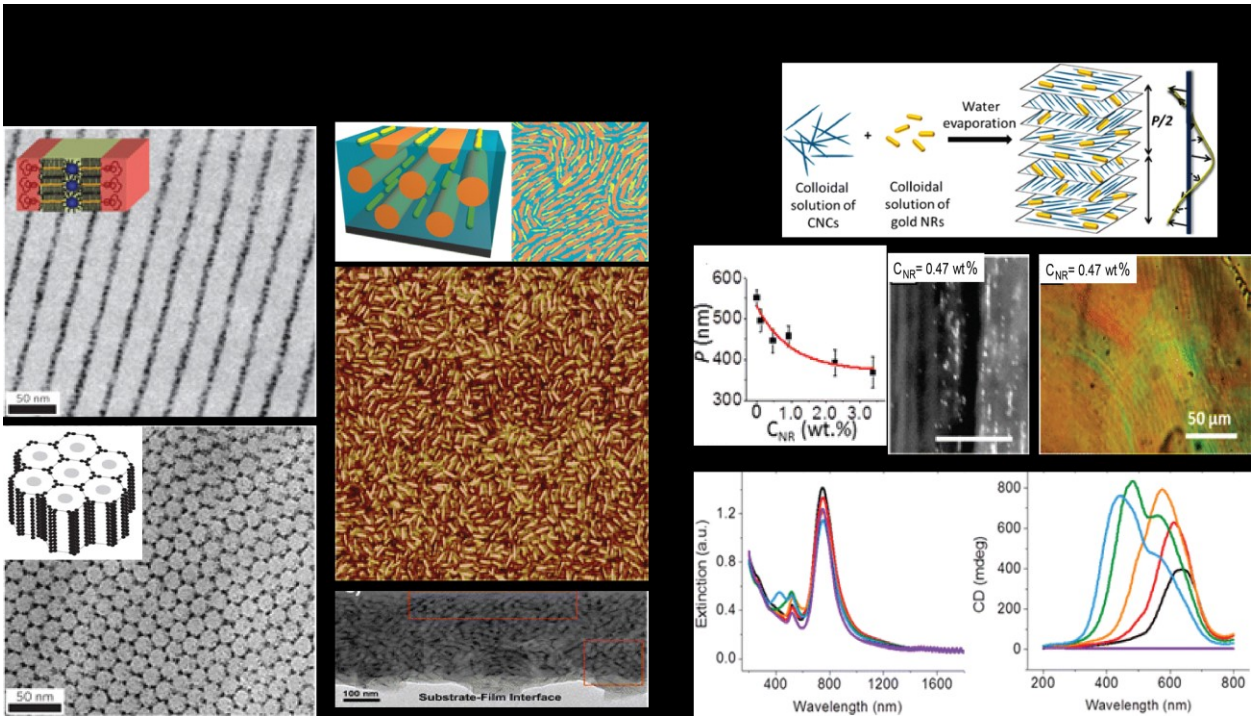

Figure 7. Formation of periodic pNCs. a) A BCP-based supramolecular matrix, PS-b-P4VP((PDP)$_r$, self-organizes into lamellar or cylinder morphologies by tuning the volume ratio of PS:P4VP(PDP). Spherical nanoparticles and nanorods selectively self-assemble into the P4VP domain due to strong attraction between the hydrophilic nanoparticles and the PMMA matrix.[75-76] Reproduced with permission from ref 75. Copyright 2012 American Chemical Society and Reproduced with permission from ref 76. Copyright 2009 Nature Publishing Group. b) Fabrication of a chiroptical pNC film by mixing aqueous suspensions of cellulose nanocrystals (CNCs) and gold nanorods. A cross-sectional SEM image of the pNC shows the nanorod (bright spots) periodically dispersed in the matrix. The helical pitch (P) depends on the loading concentration of nanorods in the pNC and NaCl content, causing changes in the circular dichrosim spectra. [NaCl loading: 0% (black), 0.02% [83], 0.06% (orange), 0.13% [84], 0.22% (blue), 2.13% (violet)]. Polarization microscopy images of the pNC show the chiral nematic nature of the film. [81-82] Reproduced with permission from ref 81. Copyright 2014 American Chemical Society and Reproduced with permission from ref 82. Copyright 2015 American Chemical Society

3.2 Nanoparticle Chains

As observed for periodic pNCs, the optical response of assembled pNCs relies largely on coupled LSPRs between closely spaced nanoparticles. pNCs where the plasmonic components are assembled into 1D chains with small interparticle spacings are an oft-targeted structure because of strong coupling along the length of the chain. The resulting plasmonic superstructure can exhibit complete charge delocalization over the entire chain or charge localization at discrete sites along the chain.[85] Nanoparticle chains can also serve as plasmon "waveguides" through which optical fields can propagate despite the physical size of the chain being much narrower than the diffraction limit.[86]

A conventional strategy for aligning plasmonic nanocomponents into a 1D structure is through the use of a polymer template. Similar to periodic pNCs where metal nanoparticles are sequestered into BCP domains, nanoparticles can also be aligned at BCP domain interfaces to produced chain-like superstructures. In a simple polystyrene-b-poly(methyl methacrylate) (PS-b-PMMA) BCP, Au nanoparticles functionalized with thioctic acid are self-organized into single particles, dimers, and nanochains by controlling the size of the PMMA block. PMMA domains modified with ethylenediamine can be linked with the acid-functionalized nanoparticles using carbodiimide cross-linking to fabricate the nanoparticle pattern with nanoscale periodicity and minimal aggregation.[87] (Figure 8a) Au nanoparticles can also be chemically conjugated to pendant groups of a polymer chain, where polymer backbone length controls chain length and the internal spacing of the pendant groups dictates interparticle spacing.[88] In this strategy, interparticle spacing is capable of reaching the close-packed limit (~ 3nm), which is dictated by ligands directly grafted onto the Au surface. (Figure 8a)

More recently, the assembly of 1D plasmonic chains has been demonstrated by selective modification of metal nanoparticle surface. For spherical metal nanoparticles, Janus-type surfaces resulting from ligand-shell defects can lead to directed assembly in a preferred

direction.[89] For anisotropic building blocks such as metal nanorods, preferential modification of either the side facets or end facets of the nanorod can direct assembly in 1D superstructures. Plasmonic nanorods have been demonstrated to assemble step-wise into chains by selective modification of nanorod ends with hydrophobic grafts[90-91] and BCP grafts that can be cross-linked.[92-93] End-to-end alignment is confirmed by a clear red-shift in the longitudinal LSPR of the nanorods, which becomes more pronounced with increased linearity of the chain. (Figure 8c) By protecting the side facets of the nanorod with a second ligand or graft, chain formation can be induced for single nanorods as well as rafts of nanorods. This assembly is the result of competition between the different aggregation states that arise from the different solubilities of the end- and side-grafts in a solvent mixture.[94] However, the majority of these 1D assemblies require further incorporation into an appropriate matrix before being classified as a true pNC.

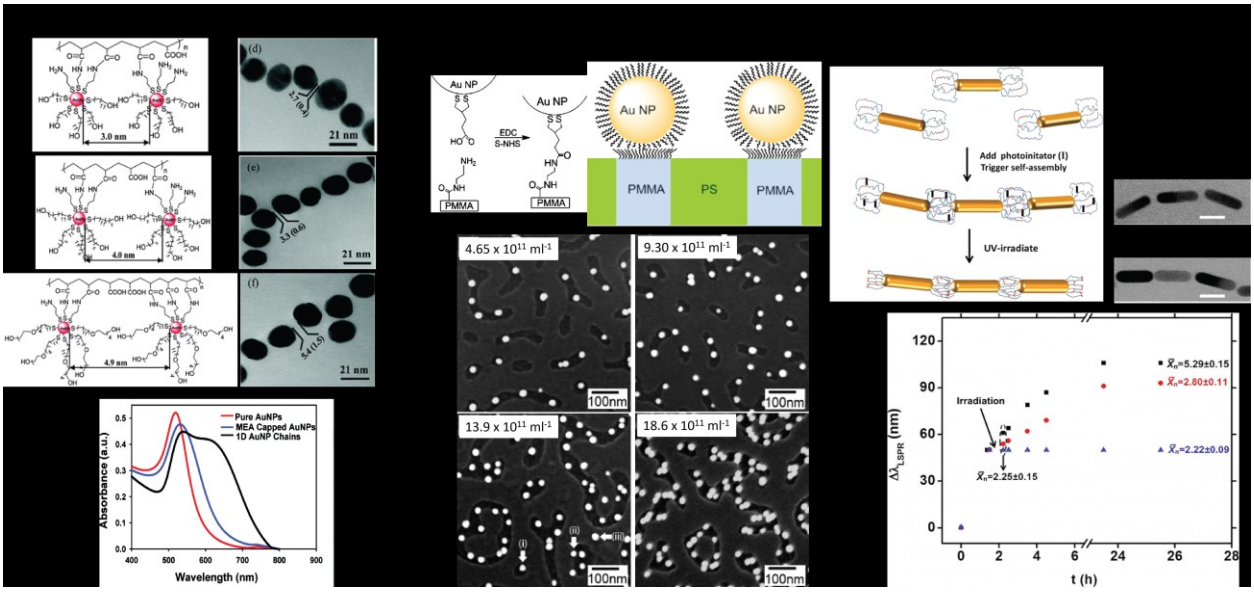

Figure 8. Three methods to control the inter-particle spacing in 1D linear nanoparticle chain. a) Amine-functionalized Au nanoparticle chains form a 1D chain by covalent attachment with the carboxylic acid groups on a polymer backbone. The interparticle spacing can be tuned by using different ligand lengths: 11-Mercapto-1-undecanol (2.7 nm), 16-hydroxy-1-hexadecanethiol (3.3 nm) and 1-mercaptoundecyl tetra(ethylene glycol) (5.4nm).The LSPR of the 1D chain shows two distinct absorption peaks at 534 nm

and 614 nm due to coupling.[88] Reproduced with permission from ref 88. Copyright 2008 American Chemical Society. b) Thioctic acid-functionalized Au nanoparticles assemble into the PMMA domain of PS-b-PMMA BCP template. The assembled nanoparticles result from cross-linking Au nanoparticles and functionalized PMMA using carbodiimide chemistry. The concentration of Au nanoparticles in the pNC can be used to change the interparticle spacing.[87] Reproduced with permission from ref 87. Copyright 2009 Institute of Physics Publishing. c) PS-co-PI BCP ligands tethered to the ends of gold nanorods induce nanorod self-assembly into 1D chains, which can then be cross-linked using a photoinitiator. The LSPR wavelength of the 1D chain depends on the number of nanorods in the chain, which is tuned by the irradiation time.[92] Reproduced with permission from ref 92. Copyright 2012 American Chemical Society.

3.3 Nanojunctions in pNCs

Nanojunctions formed by closely-spaced, non-close-packed plasmonic nanoparticles are highly desired because they exhibit high electromagnetic field confinement in their interstitial gaps. Charge density accumulation at these sites can lead to enhancement nearing 10^7 times the incident field intensity. While lithographic techniques are able to define nanostructure location with a high degree of precision, metal deposition associated with these techniques typically forms nanostructures with rough surfaces or composed of small coalescing grains.[95] As a result, these metal nanostructures rarely achieve the perfectly sharp features that are ideal for generating plasmonic nanojunctions. These surface irregularities also present a challenge when fabricating nanojunctions where metal nanostructures are separated by only a few nanometers. Self-assembly thus provides a compelling strategy for generating plasmonic nanojunctions and pNCs using a bottom-up approach.

Shaped metal nanoparticles are a primary building block for the assembly of pNC nanojunctions, since electromagnetic “hot spots” are particularly pronounced at sharp nanoscale features (i.e. the antenna effect). Anisotropic metal nanoparticles support LSPR modes where charge localization into the vertices and edges of the nanoparticle and enables strong,

orientation-dependent electromagnetic coupling. For two approaching nanoparticles, the attractive van der Waals forces scale linearly with the surface area of interaction.[96] As a result, shaped nanoparticles tend to organize into close-packed clusters that maximize this interaction (e.g. rods align side-by-side,[97] cubes align face-to-face[98-99]). One strategy to avoid close-packing and to assemble pNC nanojunctions is to selectively modify the surface of the nanoparticle components. For Au nanorods, several methods exist for selective modification of nanorod tips and can be utilized to control interparticle interactions within a pNC.[100] For example, nanorods can be selectively grafted at their tips with PS tethers and then assembled under controlled solvent conditions to promote tip-to-tip assembly. This orientation enables coupling between the longitudinal dipolar LPSR modes of each nanorod.[101] (Figure 9a)

A second strategy is to utilize the interactions of the graft polymer and matrix polymer to drive nanoparticles to adopt a preferred orientation based on minimization of entropic forces. Close-packed structures are unfavored due to steric repulsion between grafted polymer chains. Our group demonstrated that shaped nanoparticles such as Au nanorods, Ag triangular nanoprisms, and Ag nanocubes grafted with hydrophilic polymers will form oriented nanojunctions when assembled within a glassy hydrophobic PS matrix. For example, when Ag nanocubes are grafted with long poly(ethylene glycol) chains, the cubes self-organize into linear clusters where each nanocube is oriented edge-to-edge with its nearest neighbor and give rise to coupled LSPR modes localized in the nanoscale (<4 nm) gaps. [102-103] Polymer-directed assembly can achieve programmed self-assembly of metal nanoparticles into homojunctions[103] (clusters composed of plasmonic building blocks with the same size and shape) and heterojunctions[104] (clusters composed of different plasmonic building blocks) with excellent control over interparticle orientation. (Figure 9b) Moreover, the polymer matrix serves as a convenient medium for capturing desired plasmonic structures as they evolve, enabling long-term stability of the structures. A major challenge, however, is achieving precise nanojunction orientation, rather than a distribution of orientations and cluster sizes.[105-106] The morphologies of

these pNCs typically result from diffusion-limited NP assembly, since NPs must move through a high viscosity polymer medium. As a result, pNCs structures are limited to optical functions that a highly defect-tolerant or do not place a stringent requirement on periodicity.

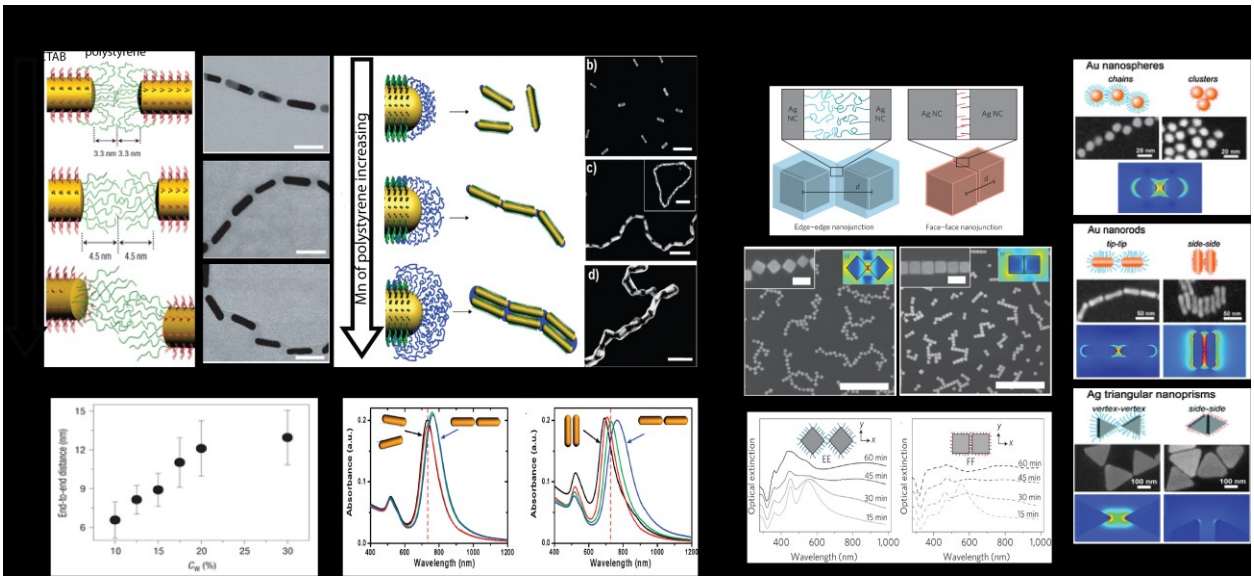

Figure 9. Two examples of controlled orientation of a nanojunction. a) Selective modification of Au nanorods. Nanorods are coated with the surfactant CTAB on the sides and thiol-terminated polystyrene chains at their ends. The orientation of nanorods in each nanojunction is tuned by the molecular weight of polystyrene.[100-101] *Reproduced with permission from ref 100. Copyright 2008 American Chemical Society and Reproduced with permission from ref 101. Copyright 2007 Nature Publishing Group. b) Entropic self-assembly of Ag nanocubes. Homogeneous polymer-coated nanocubes assemble in a PS matrix due to spontaneous phase segregation. Interparticle orientation is tuned by graft length. For longer grafts (55k PVP), the nanocubes favor edge-edge (EE) orientations due to large entropic forces stemming from graft compression. For shorter grafts (5k PEG), nanocubes prefer a face-face (FF) orientation due to strong van der Waals attraction. The EE junction possesses a highly confined electromagnetic field. This strategy also can be used to fabricate oriented nanojunctions for spherical nanoparticles and various anisotropic particles such as nanorods, and triangular nanoprisms.*[103-104] *Reproduced with permission from ref 103. Copyright 2012 Nature Publishing Group and Reproduced with permission from ref 104. Copyright 2013 The Royal Society of Chemistry.*

One potential solution is to utilize DNA constructs. With the advent of DNA origami, it has become possible to arrange plasmonic NPs into programmed nano- to mesoscale structures.[107] Kuzyk et al. formed plasmonic NP helices with spatial accuracy of 2 nm that showed both circular dichroism and optical rotary dispersion in the visible range.[108] As the sophistication of the field increases, increasingly complex and interesting geometries are becoming available[109] including NP superlattices.[110-111] While these DNA—programmed structures are still solution-dispersed d and often require buffering at specific ionic strengths to stabilize DNA, the ability to backfill these structures with polymers or solubilize DNA constructs in polymer solutions has the potential for integrating these NP assemblies into large-scale pNC materials.

4. Responsive pNCs

There is growing interest in creating reconfigurable pNCs capable of modulating their optical response upon being triggered by an external stimulus. The underlying philosophy for creating reconfigurable pNCs has therefore been to develop strategies to modulate one or more of the following material or geometric parameters in a reproducible and reversible manner: (i) the spatial organization of the pNC, (ii) nanoparticle/nanostructure shape, and [112] the dielectric constant of the pNC matrix. The former strategy provides several means of generating responsiveness, since optical function is highly dependent on the separation distance (i.e. gap) between plasmonic components, their absolute and relative orientation (in case of anisotropic particles), and any hierarchical configuration into larger assemblies.

Apart from a handful of studies demonstrating top-down fabrication combined with MEMS-based actuation of plasmonic nanostructures,[113] reconfigurable pNCs require precise control over nanostructure assembly. Significant advances have been made in developing new and modifying already-existing strategies for reconfiguration involving temperature, electrical, and mechanical triggers to actively modulate the optical properties of pNCs. Below we outline

some of the most prominent strategies, categorized in terms of the parameters they modulate.

4.1 Modulation of Plasmonic Gaps

The evanescent near-field associated with LSPR excitation decays exponentially with distance from metal surfaces. This effect is pronounced for plasmonic particles and surfaces that are separated by gaps <100 nm. Thus, a simple yet effective strategy for modulating the optical response of pNCs is altering the separation distance between plasmonic nanocomponents in the composite material.

An intuitive approach involves stretching an elastomeric substrate containing immobilized metal nanoparticles to simultaneously increase the distance between nanoparticles in roughly the same proportion as the applied strain. One of the first demonstrations of this approach in pNCs was with ~100 nm Au nanostructures (bowties and rods) patterned via nanostencil lithography with sub-50 nm gaps onto a flexible elastomer film.[114] By applying a mechanical strain (5%) to the nanorod-polymer composite in the direction perpendicular to the longitudinal axes of the rods, measurable shifts in the transmission spectra could be obtained. Arguably, the magnitude of such optical shifts could be improved by shrinking the initial gap between the nanostructures; however, the generation of small <10 nm gaps is limited by the resolution limit of top-down patterning methods. Similar stretching-based approaches have been used for creating responsive pNCs containing Au semishells[115] and nanospheres,[116] with the potential for immediate application as strain sensors.[57] The stretching of pNCs was also recently used to create multiplexed metasurface holograms wherein the hologram switches from one image to another with increasing strain.[117] This was achieved by depositing a pattern of Au nanorods into a stretchable elastomer film that yielded more than one hologram at different image planes. By optimizing the nanorod pattern, the authors were able to achieve up to three multiple holograms appearing at the same image plane at three different values of strain.

Another approach to modulating gap distances is by grafting nanoparticles with polymer

chains capable of undergoing drastic conformational changes in response to a trigger. Conformation changes can alter the steric repulsion between the grafts, leading to a change in the equilibrium separation distance between the nanoparticles. Poly (N-isopropylacrylamide) (pNIPAM) is an excellent candidate for this task, as it exhibits a lower critical solution temperature (LCST) in water, whereby its chains undergo a drastic transition at ~33^{o}C from an extended to a collapsed state upon increasing temperature.[118] This approach has now been applied to a variety of plasmonic nanoparticle systems.[119] An elegant implementation of this strategy[120] used visible light to trigger solution-dispersed Au nanoparticles grafted with pNIPAM chains. Photothermal heating from LSPR excitation caused the local temperature to exceed the LCST followed by pNIPAM brush collapse, triggering the aggregation of the nanoparticles into clusters. Cooling the solution below the LCST then caused immediate dissociation of the clusters. This association-dissociation process was shown to be fully reversible over a large number of cycles. While this strategy was applied in a solution, it would be useful to extend it to a more robust polymeric platform. Other stimuli-responsive polymers such as poly(2-vinylpyridine) which is sensitive to solution pH have also been successfully used for actively modulating the gap between plasmonic nanoparticles.[121]

Introducing stimuli-responsive bonding motifs in the grafts may also dynamically alter the interactions between plasmonic nanoparticles. While this can be readily achieved using mutually complementary single-stranded DNA grafts,[122] synthetic polymer-based approaches offer a more robust end product for optical applications. An example of such an approach involves Au nanoparticles grafted with PS chains terminating in either diaminopyridine or thymine units, which only form complementary hydrogen bonds at low temperatures.[123] By mixing nanoparticles functionalized with the two kinds of units, the nanoparticles could be made to assemble into ordered lattices at low temperatures, where an increase in temperature caused the structures to disassemble. A major challenge for employing these reversible nanoparticle interactions in pNCs is the ability to encapsulate the nanoparticles into a polymer or soft matrix

that allows for nanoparticle motion.

4.2 Modulation of Orientation

The optical response of pNCs is sensitive to the *absolute* orientation of the embedded nanocomponents due to the polarization of the incident light and the directional nature of its impingement. (Figure 10A) While nanoparticles — especially anisotropic nanoparticles — can be suitably surface-functionalized to self-assemble into highly oriented configurations, reconfiguring these orientations to modulate the optical response is very challenging.

One solution is to use a liquid crystal (LC) medium that exhibits strong alignment over macroscopic length scales, thus providing an additional driving force for orienting and organizing the pNC. (Figure 10B) Moreover, many LCs exhibit order-disorder transitions with respect to temperature and can be readily aligned by mechanical shear, electric field, and even magnetic field. In this manner, LC-based pNCs have the potential to transduce external fields into optical response. Surfactant-based lyotropic LCs have been successfully used to organize Au nanorods and to realign them.[124] In one example, the nanorods form the core of the LC hexagonal columnar phase, which in turn exhibits long-range nematic order. The ordered Au nanorods were found to exhibit strong polarization sensitivity and could be realigned via external shear or strong magnetic fields. To enable easier realignment of nanoparticles in LCs with weak electric fields, Zhang et al. used a thermotropic mesogen and functionalized Au nanorods with a surface-anchoring surfactant. This led to nanorod alignment perpendicular (rather than parallel) to the LC director.[125] A complementary approach to assembling LC-based pNCs involves using LC molecules as grafts for the nanoparticles instead of using them as the medium.[126-129] The natural propensity of these molecules to assemble into aligned phases effectively introduces anisotropic interactions between otherwise spherically-symmetric nanoparticles, facilitating their overall ordering into smectic, hexagonal, and lamellar phases. These systems have also been demonstrated to re-align in response to shearing or heating/cooling.

The *relative* orientation between anisotropic plasmonic nanoparticles is also a key factor affecting the optical response as it directly determines the type of LSPR modes that participate in coupling. Modulating the relative orientation of shaped nanoparticles within pNCs is challenging, as orientation must typically be controlled over multiple nanoparticle pairs with precision. A promising approach evolves from our own work on polymer-grafted Ag nanocubes in polymer thin films where we observed that the grafting conditions (e.g. graft density, length, and conformation), govern steric repulsion between grafts and, thus, dictate the relative orientation of nanocubes.[102-103] (Figure 10C) In particular, weak and strong grafting conditions promote face-to-face (FF) and edge-to-edge (EE) configurations, respectively. We also demonstrated that temperature could be used to switch from EE to FF configurations, albeit irreversibly. The potential exists for stimuli-responsive polymer grafts capable of undergoing reversible swelling-shrinking behavior to instigate similar nanoparticle orientation switching. However, if the end goal is to attain a transition between a disordered and an oriented configuration of NPs, then simpler approaches such as uniaxial stretching of pNCs may be sufficient. For instance, Pletsch et al. demonstrated that the uniaxial elongation of an elastomeric polymer originally carrying randomly-oriented Au nanorods oriented the nanorods in the direction of stretching, and that the resulting optical spectrum displayed polarization dependence upon stretching.[130] Gao et al. also demonstrated a pNC of ordered Au nanodisks on an elastomeric polymer that shifted optical resonances over a range of 600 nm by uniaxial stretching.[131]

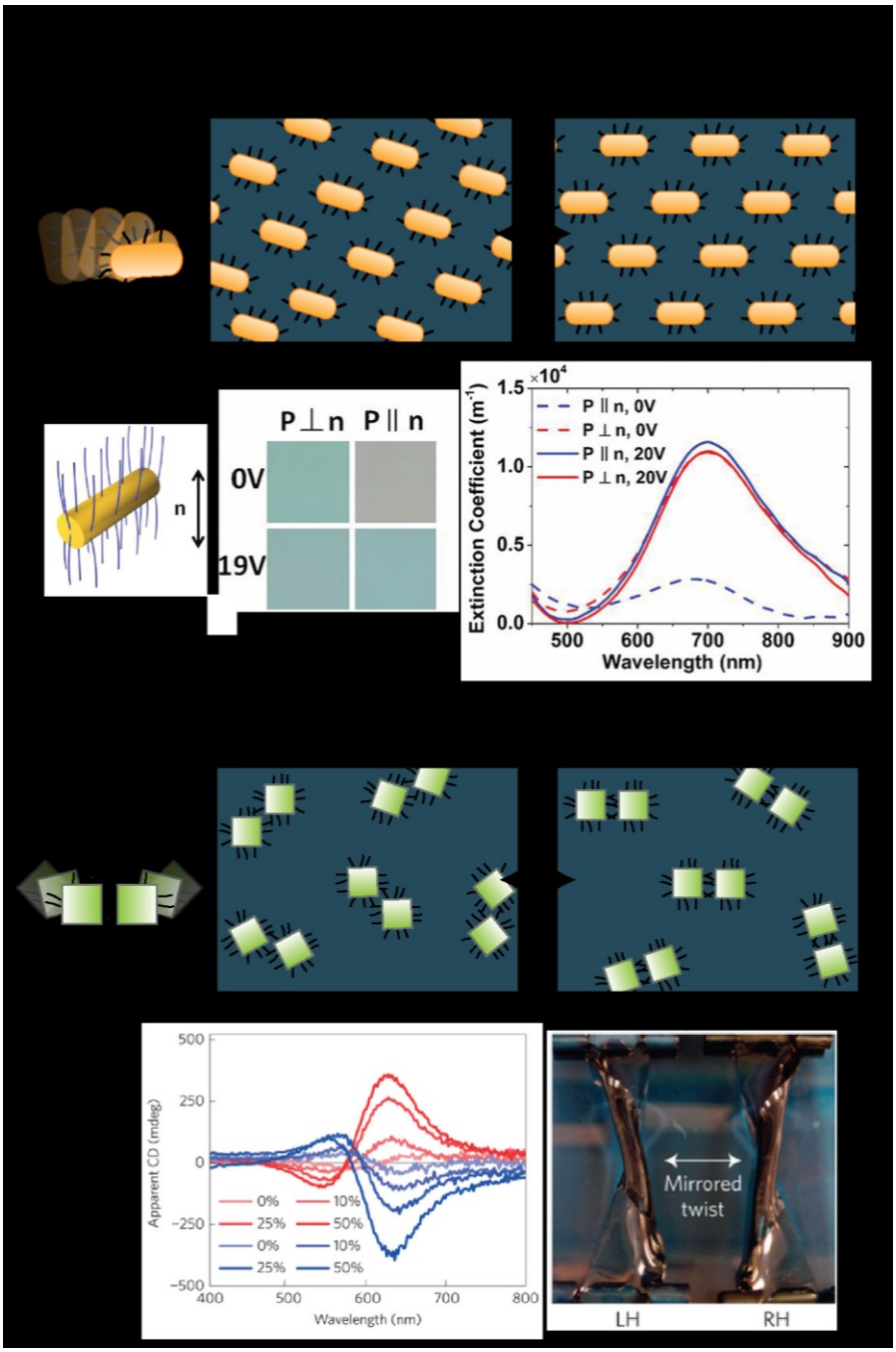

Figure 10. Schematic of responsive pNCs exhibiting changes in absolute orientation versus relative interparticle orientation. a) Absolute orientation typically requires realignment of plasmonic components across the entire pNC. b) Nanorods aligned in a nematic liquid crystal host of 5CB respond to changes in voltage, where the host serves as the director of orientation. The optical response of the pNC is observed by a physical color change in the material with respect to both voltage and polarization.[125] Reproduced with permission from ref 125. Copyright 2015 American Chemical Society. c) Changes in the relative

orientation of a pNC involve local changes in relative angles of plasmonic components. The pNC in d) responds to mechanical twist deformations, which causes Au nanorods to adopt chiral structures where nanorods are oriented at varying angles relative to each other. The resulting pNC exhibits varying circular dichroism response.[122] Reproduced with permission from ref 122. Copyright 2016 Nature Publishing Group.

A more complex modulation of optical response, though not necessarily the most difficult to implement, involves larger-scale rearrangement of the higher-order configuration of plasmonic nanoparticles. One such rearrangement involves changes in chirality, which could lead to interesting and useful polarization rotation effects. This is best illustrated by the recently developed pNC created by coating multiple layers of plasmonic nanoparticles onto a twisted elastomer film.[122] (Figure 10D) The subsequently relaxed film exhibited unique chiroptical activity upon stretching that was attributed to S-shaped nanoparticle chains formed in the pNC. These S-chains exhibit a non-planar buckled geometry that reversibly change their chirality upon stretching and relaxing. A more drastic rearrangement involves structural phase transitions from one ordered periodic phase to another, akin to those observed in metal alloys and oxides. The closest relevant phase transition achieved for a nanocomposite was demonstrated with Au nanoparticles grafted with promesogenic ligands, which led to transitions between well-defined smectic, rectangular columnar, hexagonal columnar and isotropic phases.[126] Due to the small size of the nanoparticles, the LSPR response was weak; however, such an approach seems promising for creating switchable pNCs using more appropriate nanoparticle building blocks.

4.3 Modulation of pNC Components

The approaches described above all involve changes in the structural configuration of pNCs. We next discuss the remaining few approaches that involve altering the intrinsic optical response of either the plasmonic nanocomponents or the dielectric pNC medium, which provide two additional knobs for tuning pNC properties.

A classic example of a responsive optical nanocomposite where the plasmonic building blocks are fundamentally altered are photochromic glasses, where AgCl undergoes reduction by ultraviolet light to produce Ag^0 and an opaque composite. Reversible oxidation back to AgCl produces a transparent composite. In a similar vein, photochromic behavior can be engineered into pNCs by changing metal nanoparticle size and shape. For example, laser excitation can be used to convert well-aligned Ag nanorods into spheres within a PVA matrix.[132] The approach was inspired by an earlier observation that small Au rods molten by pico- and nanosecond laser irradiation recrystallized as spheres.[133] The simplicity of the approach and the ability to write with different degrees of polarization (rod versus sphere content) allows for multiplexed optical sensing. Nanosecond laser pulses were also recently used to organize plasmonic nanoparticles in polymers.[134] Specifically, the optical forces arising from interference of the pulses were used to manipulate nanoparticles within the polymer. Such capacity to write and erase plasmonic patterns was used to demonstrate rewritable photonic crystals, optical elements, and 3D holograms.

The dielectric constant of the pNC medium is most intuitively manipulated by altering the polar or charged character of its functional groups. Ledin et al. achieved such modulation by designing pNCs containing Au nanorods of a controlled aspect ratio and a solution-processable electroactive and electrochromic polymer containing thiophene.[135] The oxidation state of the thiophene group, and thereby the dielectric function of the polymer, could then be modulated by an externally applied electric field, resulting in reversible LSPR modulation of up to 25-30 nm. A subtler approach involves changing the isomerization state of molecules in the medium. This was achieved by grafting azobenzene-silsesquioxane conjugates onto Au nanocubes deposited on a quartz substrate.[136] The refractive index of the resulting Au-polymer thin film could then be modulated reversibly via ultraviolet and visible light, which caused transitions between the cis and trans states of the azobenzene moieties.

5. Interfacial Plasmonic Composites

A large motivation for the discovery and study of novel plasmonic materials is the development of flat optical components[137] for application in optical coatings, ultra-thin or flexible photovoltaics, and high-resolution imaging and lithography. To meet these needs, a new class of composite materials has emerged, which we term *plasmonic interfacial nanocomposites (pINCs)*. Classical interfacial composite materials are defined as interfaces that are composed of multiple components, where each component maintains a distinct property (e.g. particle size, phase) but contributes to a collective interfacial property,[138] such as miscibility or chemical function. Examples include bubbles that gather at liquid-air interfaces and reverse osmosis membranes comprised of binary polymer blends. Here, we define pINCs as interfacial nanocomposites that exhibit collective optical behavior. Unlike bulk pNCs, the optical response generated by pINCs is confined to a nanoscale boundary layer.

This classification stems from the inherently different electromagnetic response exhibited by plasmonic components when placed at an interface versus in a bulk material. A simple example is a spherical Ag nanoparticle that is encapsulated by a polymer matrix. (Figure 11) When located in the bulk polymer, the nanoparticle supports a dipolar LSPR that can be excited by incoming light at any angle; the resulting electromagnetic near-field is maximized in the direction parallel to the polarization direction of the incoming light wave. If the same Ag nanoparticle is now situated at the surface of the polymer (i.e. the air-polymer interface), the plasmon response is fundamentally altered. The nanoparticle now supports two LSPRs, one where the majority of the near-field is located at the Ag-air interface and one where the majority of the near-field is located at the Ag-polymer interface. The resulting near-field intensities are now dependent on both the polarization of the incoming light wave as well as the angle of illumination with respect to the air-polymer interface. Figure 12A shows a finite difference time domain (FDTD) simulation of the near field around an Ag nanocube at the interface of a

dielectric material. There are two resonance peaks for the system, one in which the near field is strongest at the Ag-air interface, the other at the Ag-dielectric interface.[139]

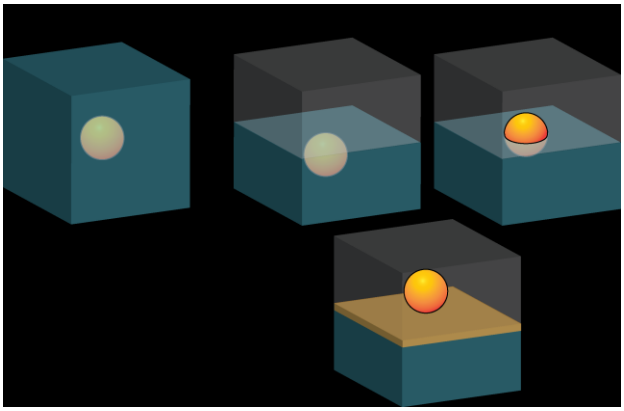

Figure 11. Schematic of a nanoparticle located in a bulk, homogeneous matrix and of a nanoparticle located at three different kinds of interfaces.

Here, we discuss three unique interfacial structures that have emerged as pINCs: (i) particles at the interface, (ii) nanoparticles on a 2-D material, and [112] nanoparticles coupled to a metallic backplane. An important distinction that we have made in identifying these pINCs is that the resulting plasmonic response is not a superposition of the response stemming from the plasmonic component and the interface.

5.1 Nanoparticles at an Interface

The simplest pINC structure that can be identified is a plasmonic nanoparticle that is located at the interface between two different dielectric media. As described in the previous section, such pINCs exhibit distinctly different surface plasmon behavior than in bulk pNCs due to the anisotropic environment imposed on the nanoparticle.

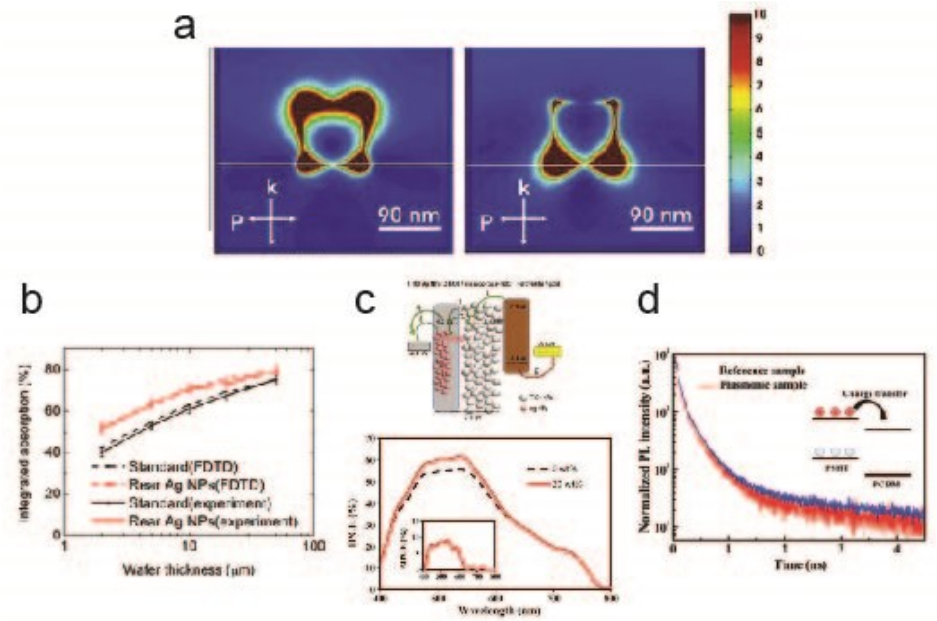

Figure 12 a) FDTD simulations showing the nearfield intensities for resonance peak at Ag-air interface and Ag-dielectric interface.[139] Reproduced with permission from ref 139. Copyright 2005 American Chemical Society. b) Experimental and simulated integrated absorption of standard Si cells (black) and cells with Ag nanoparticles at the back interface[140] Reproduced with permission from ref 140. Open access under a CC BY license. c) Schematic energy diagram for carrier transport in perovskite solar cells with Ag nanoparticles and Incident photons to current efficiency (IPCE) plot as a function of incident light without (black) and with Ag nanoparticles.[141] Reproduced with permission from ref 141. Copyright 2016 Elsevier, Ltd. d) PL decay profiles for bulk heterojunction cell without (blue) and with plasmonic nanoparticles.[142] The decay indicates strong coupling between the plasmon and excitons, which facilitates exciton dissociation. Reproduced with permission from ref 142. Copyright 2011 American Chemical Society.

These interfacial structures are primarily exploited for two purposes. The first is to increase light trapping and photoabsorption within a medium by using plasmonic components to direct light scattering within a dielectric layer. Plasmonic nanoparticles located at a dielectric interface support LSPR modes that can focus intense near-fields into an underlying layer, as

observed in single-particle darkfield spectroscopy experiments for Ag nanocubes on a glass substrate.[139] Optical scattering resulting from this LSPR excitation can be used to effectively trap light near the interface. Consequently, these pINCs have been widely exploited to improve the photon conversion efficiency of photovoltaic cells that suffer from poor photoabsorption, such as thin-film devices.[143-145] Figure 12B shows the absorption of a thin film Si solar cell with the traditional Al back reflector and with hemispherical Ag nanoparticles embedded in SiO_2 between the Ag reflector and Si layer. Amorphous Si cells,[140,146-148] and bulk heterojunction cells also utilize pINCs. In the latter case, pINCs can be integrated into the device at the active anode[112] or into the electron or hole blocking buffer layers that sandwich the photoactive layer.[149-150] The subject of plasmonic solar cells has been well covered in the previous review by Jang et al.[151] While the increase in absorption for solar pINCs is promising, there is an inherent trade-off that limits the utility of these materials. As surface coverage of the plasmonic components is increased, reflectance increases and quenching of the active material can occur. At high NP concentrations, the inclusion of a pINC layer can be detrimental to device performance. Thus, each pINC must be optimized not just for maximum absorbance, but for maximum conversion efficiency.

Second, these pINCs are platforms for hot electron generation, where LSPR decay occurs via electron excitation and charge transfer into a semiconductor layer. Nanoparticle size and shape are critical parameters in these pINCs, since nanoparticle morphology has a profound effect on whether LSPR decay occurs radiatively or non-radiatively. Non-radiative decay pathways tend to dominate for pINCs comprised of small metal nanoparticles that exhibit large optical absorption cross-sections at the LSPR wavelength. Several examples of these pINCs consist of Ag nanoparticles at a TiO_2 interface where excitation of LSPRs associated with the nanoparticles results in hot electron injection into the TiO_2 layer,[152-153] followed by in Ag oxidation due to electron depletion. In photovoltaic devices where plasmonic nanoparticles are incorporated into the buffer layer, pINCs can be utilized for controlling both charge separation

and photoabsorption.[141,154-160] Figure 12C shows the schematic energy diagram for carrier transport in perovskite/Ag solar cells, which undergo improvement of about 10% in internal photoconversion efficiency. In organic solar cells, pINCs have also been demonstrated to enhance fluorescence intensity and rate of exciton generation of 20 to 30 percent while reducing the lifetime of photogenerated excitons.[142] (Figure 12D) Similar use of pINCs has been demonstrated for photocatalysis, as detailed in a recent review by Clavero.[152] The increase in efficiency observed by the addition of pINCs is promising but not necessarily cost-effective for a solar industry with an eye on decreasing device cost. New plasmonic materials such as Cu-based or graphene may be able to exploit plasmonic enhancement effects with a lower cost per Watt.

Aside from cost, a critical challenge for designing pINCs is the ability to control location of the NPs at the interface. In many cases, It is unclear whether the NPs reside at the true interface or whether the interface is inherently distorted by the presence of the plasmonic NP. Conformal passivation of the NP by atomic layer deposition or layer-by-layer deposition, or the use of core-shell plasmonic NPs may serve as effective means to mitigate these effects.

5.2 Nanoparticles and Two-Dimensional (2D) Materials

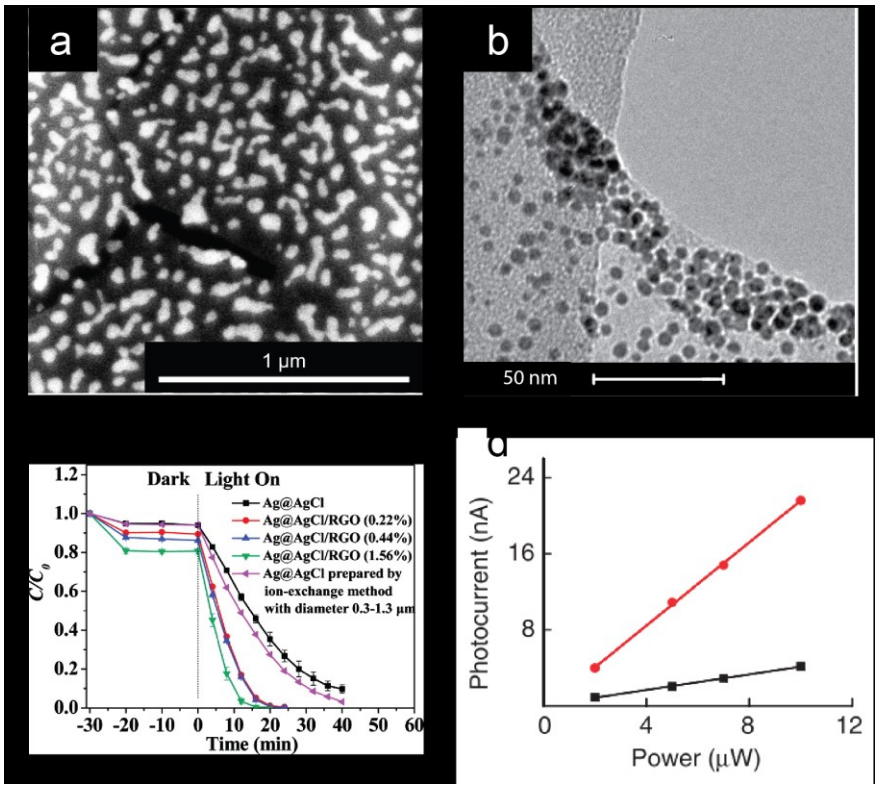

Figure 13. a) SEM image of Ag nanoislands formed on the surface of graphene.[83] Reproduced with permission from ref 83. Copyright 2012 National Academy of Sciences. b) TEM images of Au nanoparticles affixed to 1-pyrenebutyrate functionalized graphene[161] Reproduced with permission from ref 161. Copyright 2010 American Chemical Society. c) Change in RhB concentration as a function of irradiation time under visible light with different photocatalysts.[162] Reproduced with permission from ref 162. Copyright 2011 American Chemical Society. d) Photocurrent generated as a function of laser power for typical graphene photodetector (black) and one with Au nanoparticles attached [163] Reproduced with permission from ref 163.Open access under a CC BY license.

Plasmonic composites fabricated by integrating plasmonic nanoparticles and 2D materials such as graphene are novel pINCs that are attracting significant attention due to their unique physiochemical properties. 2D pINC structures are primarily fabricated by physical deposition methods onto 2D substrates or by the attachment of colloidal metal nanoparticles. In a simple

demonstration of 2D pINCs, Xu et al. carried out Au evaporation to form metal islands on top of monolayer graphene.[83] (Figure 13A) Using analytes deposited onto the graphene side of the pINC, they observed that surface-enhanced Raman scattering signals were more robust and reproducible due to the atomically smooth surface and uniform analyte adsorption afforded by the flat graphene surface. pINCs can be fabricated by loading plasmonic nanoparticles directly onto chemically modified surfaces of the 2D material, either through chemical linkers or electrostatic interactions. For example, dispersions of graphene sheets functionalized with 1-pyrenebutyrate (which imparts a negative charge to graphene) mixed with positively charged Au nanoparticles results in spontaneous assembly of the two components. (Figure 13B) The resulting pINC, which displays higher nanoparticle loading densities at the graphene edges, exhibits electrocatalytic behavior indicative of stable and intimate electrical contact between the two materials.[161] In chemical attachment methods, nanoparticle loading can be controlled by the volume of nanoparticles in a mixed dispersion[164-165] or by treating the 2D materials with an adhesion layer to create a homogenous dispersion.[163,166] Plasmonic nanoparticles can also be directly nucleated onto the 2D sheets.[162,167] Immobilization of nanoparticles onto 2D materials serves to mitigate nanoparticle aggregation and maintain controlled interparticle separation distances for specific optical functions.[168]

Importantly, 2D materials can serve as an active optoelectronic component in a pINC. For plasmonic components attached to semiconducting 2D layers, the pINC interface produces a Schottky barrier that promotes charge transfer between the 2D material and the metal, accelerating photoinduced electron-hole separation. Hot electrons generated by LSPR excitation can transfer rapidly to the 2D materials, as observed for Ag nanoparticles deposited onto reduced graphene oxide[162] and Ag nanoparticles on CoS sheets.[165] pINC photocatalysts show an improvement of photodegradation rate up to four fold over nanoparticles alone (Figure 13C) and are also stable over several recycle experiments. Graphene coupled to plasmonic arrays have been demonstrated to exhibit plasmon-enhanced photocurrent generation.[163,169]

Plasmonic Au nanoparticles attached to ultrathin 2D MoS_2 layers have already been demonstrated as improved electron and hole transport layers in bulk heterojunction photovoltaic cells, where the MoS_2 does little to alter the plasmon response of the Au nanoparticle components.[163,167] In the case of a graphene-based photodetector (Figure 13D), the current generated for a pINC device loaded with Au nanoparticles is 4 to 5 times higher than graphene alone.

However, while these 2D pINCs exhibit potential as multifunctional materials with improved optoelectronic functions, application of these materials is inherently linked to the ability to nanomanufacture these pINCs at-scale and with high quality. Many of the reported pINCs to-date have been demonstrated with small flakes of the 2D material. Translation of these pINCs to large-area 2D sheets may fundamentally change both device performance and the ability to pattern the pINC, since NP anchoring sites are typically associated with defect sites of the 2D materials.

5.3 Nanoparticles Coupled to a Backplane

Recent exploration in optical metasurfaces has led to a new pINC structure consisting of metal nanostructures that are placed near a metal surface, or backplane. In this configuration, the plasmonic nanoparticle is optically coupled with the backplane, resulting in a strong optical resonance associated with the interstitial gap between the two components. Previously, lithographic structures with similar designs were demonstrated as metamaterials that absorbed frequencies from THz to IR.[170-172] This established knowledge provides important design guidelines for producing strongly absorbingpINCs. Colloidal pINCs are able to provide a low-cost, scalable alternative to lithographically produced structures Colloidal metasurfaces, where synthesized metal nanoparticles are deposited or assembled onto a metal surface, have been demonstrated to exhibit extraordinary optical absorbance.[173] For example, electromagnetic

coupling of colloidal Ag nanocubes to an Au film results in a waveguide cavity mode whose optical properties can be tuned by an ultrathin polymer spacer.[174] (Figure 14A) These colloidal pINCs have been shown to create near-perfect absorbers for incident angles up to 50°[175] and for wavelengths that can be tuned from the visible to mid-IR wavelengths by controlling plasmonic coupling between Ag nanocubes.[176] (Figure 14B)

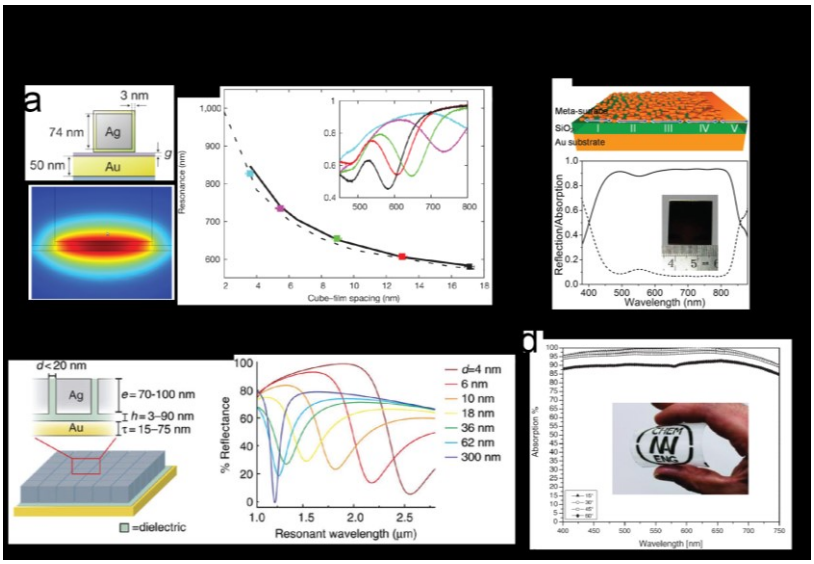

Figure 14. a) Geometry used in FDTD simulation showing magnetic field for mode formed in the gap between Au film and Ag nanocube. Position of the resonance as a function of spacer thickness.[173] Reproduced with permission from ref 173. Copyright 2012 Nature Publishing Group. b) Schematic of close packed Ag nanocube film and reflectance spectra of simulated arrays of cubes with varied interparticle spacing.[176] Reproduced with permission from ref 176.Open access under a CC BY license. c) Schematic of metallic film formation by controlled sputtering and Absorption (solid) and reflection (dotted) achieved from composite.[177] Reproduced with permission from ref 177. Copyright 2015 American Chemical Society. d) Absorption spectra of perfect composite absorber at varying angles of incidence. The inset shows the flexible composite absorber.[178] Reproduced with permission from ref 178. Copyright 2011 Wiley Periodicals, Inc.

The versatility and tunability of these nanoparticle-on-metal pINCs show great promise for future devices that require strong absorption of a narrow wavelength range. Broadband absorption requires a different approach. Highly ordered arrays of cubes can lead to multimodal composites[179] and the use of thermal annealing to create polydisperse particle size distributions can lead to a wider absorption band.[177,180] (Figure 14C) Zhou et al. designed a pINC absorber by assembling metal nanoparticles onto a nanoporous template, with a measured absorbance of 99% across the wavelengths from 400 nm to 10 μm.[181] Another method for achieving broadband absorbance is to couple a bulk pNC layer to a metal backplane. For example, by co-sputtering a metal and polymer pNC on a metal thin-film and controlling nanoparticle size and fill factor, the optical response of the resulting pINC can be tuned from a highly conducting transparent material[182] to a perfect black absorber[178] through impedance matching. (Figure 14D) Such a design has been shown to be effective for composites containing Ag, Au and Cu nanoparticles.[145,183-184] By using a photoswitchable polymer as the polymer matrix material, the optical absorption and transmission of the pINC can be further tuned upon irradiation of UV light.[185] These composites can easily be designed with solar applications in mind. pINC materials such as these have the potential for use in photocatalysis,[186] multispectral imaging,[187] selective thermal emissivity,[188] directional high quantum yield emission,[189-190] and photovoltaics.[191]

Of all the pINCs, the NP-on-metal absorbers are perhaps the most mature and well-studied nanocomposite structure. The layer-by-layer techniques used to fabricate these pINCs have proven to be successful over large-scales within a variety of platforms, such as chemical sensing.[106,192] In contrast to other pINCs, NP-on-metal absorbers have also been demonstrated with non-precious metals. In addition, the ability to control the geometric parameters of the optical gap characteristic of these pINCshas the potential to allow fundamental studies of optical device physics, such as quantum plasmonic effects and hot electron generation.

6. Conclusions and Outlook

This review illustrates the major concepts in the synthesis, fabrication, and structuring of pNCs as well as their development for various optical applications. We introduce the classification of interfacial pNCs to clearly distinguish pNCs that function only at dielectric or dielectric/metal interfaces and are likely to lead to new developments in metasurfaces, ultra-thin optical coatings, layer-by-layer device integration.

In each of the pNC types discussed, the precision assembly of nanostructures is a limiting factor in engineering advanced, state-of-the-art pNCs that rival top-down produced materials. Even the simplest nanocomposite possesses chemical and structural complexities for which no complete framework exists for predicting materials behavior. This presents a major impediment for the development of multifunctional or responsive pNCs, where nanostructure arrangement and function must be highly regulated. At the same time, it provides an excellent opportunity for new theory-informed frameworks for understanding, tailoring, and rationally engineering how nanostructures self-assemble and perform within a complex, hierarchical pNCs at multiple relevant scales.

7. Acknowledgements

The authors acknowledge the National Science Foundation (Grant CMMI-1636356) for support of this work. A.R.T. also acknowledges the National Science Foundation (Grant CHE-1508755) and the Defense Advanced Research Projects Agency (Grant W911NF-16-2-0156) for support of this work.

8. References Cited

(1) Yagil, Y.; Yosefin, M.; Bergman, D. J.; Deutscher, G.; Gadenne, P. *Scaling Theory for the Optical Properties of Semicontinuous Metal Films*, *Phys. Rev. B* **1991**, *43*, 11342-11352.

(2) Le Ru, E. C.; Grand, J.; Sow, I.; Somerville, W. R. C.; Etchegoin, P. G.; Treguer-Delapierre, M.; Charron, G.; Félidj, N.; Lévi, G.; Aubard, J. *A Scheme for Detecting Every Single Target Molecule with Surface-Enhanced Raman Spectroscopy*, *Nano Lett.* **2011**, *11*, 5013-5019.

(3) Adams, S. M.; Campione, S.; Caldwell, J. D.; Bezares, F. J.; Culbertson, J. C.; Capolino, F.; Ragan, R. *Non-Lithographic Sers Substrates: Tailoring Surface Chemistry for Au Nanoparticle Cluster Assembly*, *Small* **2012**, *8*, 2239-2249.

(4) Leonhardt, U. *Optical Metamaterials: Invisibility Cup*, *Nat. Photonics* **2007**, *1*, 207-208.

(5) Yu, N.; Capasso, F. *Flat Optics with Designer Metasurfaces*, *Nat. Mater.* **2014**, *13*, 139-150.

(6) Hofmeister, H.; Drost, W. G.; Berger, A. *Oriented Prolate Silver Particles in Glass - Characteristics of Novel Dichroic Polarizers*, *Nanostruct. Mater.* **1999**, *12*, 207-210.

(7) Selvan, S. T.; Hayakawa, T.; Nogami, M.; Kobayashi, Y.; Liz-Marzan, L. M.; Hamanaka, Y.; Nakamura, A. *Sol-Gel Derived Gold Nanoclusters in Silica Glass Possessing Large Optical Nonlinearities*, *J. Phys. Chem. B* **2002**, *106*, 10157-10162.

(8) Cai, W. P.; Zhang, Y.; Jia, J. H.; Zhang, L. D. *Semiconducting Optical Properties of Silver/Silica Mesoporous Composite*, *Appl. Phys. Lett.* **1998**, *73*, 2709-2711.

(9) Wang, P. W. *Formation of Silver Colloids in Silver Ion-Exchanged Soda-Lime Glasses During Annealing*, *Appl. Surf. Sci.* **1997**, *120*, 291-298.

(10) Zhang, J.; Dong, W.; Sheng, J. W.; Zheng, J. W.; Li, J.; Qiao, L.; Jiang, L. Q. *Silver Nanoclusters Formation in Ion-Exchanged Glasses by Thermal Annealing, Uv-Laser and X-Ray Irradiation*, *J. Cryst. Growth* **2008**, *310*, 234-239.

(11) Fang, J.; Cao, S. W.; Wang, Z.; Shahjamali, M. M.; Loo, S. C. J.; Barber, J.; Xue, C. *Mesoporous Plasmonic Au-Tio2 Nanocomposites for Efficient Visible-Light-Driven Photocatalytic Water Reduction*, *Int. J. Hydrogen Energy* **2012**, *37*, 17853-17861.

(12) Som, T.; Karmakar, B. *Surface Plasmon Resonance in Nano-Gold Antimony Glass-Ceramic Dichroic Nanocomposites: One-Step Synthesis and Enhanced Fluorescence Application*, *Appl. Surf. Sci.* **2009**, *255*, 9447-9452.

(13) Som, T.; Karmakar, B. *Nanosilver Enhanced Upconversion Fluorescence of Erbium Ions in Er3+: Ag-Antimony Glass Nanocomposites*, *J. Appl. Phys.* **2009**, *105*.

(14) Som, T.; Karmakar, B. *Surface Plasmon Resonance and Enhanced Fluorescence Application of Single-Step Synthesized Elliptical Nano Gold-Embedded Antimony Glass Dichroic Nanocomposites*, *Plasmonics* **2010**, *5*, 149-159.

(15) Som, T.; Karmakar, B. *Nano Silver:Antimony Glass Hybrid Nanocomposites and Their Enhanced Fluorescence Application*, *Solid State Sci.* **2011**, *13*, 887-895.

(16) Zhang, F.; Braun, G. B.; Shi, Y. F.; Zhang, Y. C.; Sun, X. H.; Reich, N. O.; Zhao, D. Y.; Stucky, G. *Fabrication of Ag@Sio2@Y2o3:Er Nanostructures for Bioimaging: Tuning of the Upconversion Fluorescence with Silver Nanoparticles*, *J. Am. Chem. Soc.* **2010**, *132*, 2850-+.

(17) Gunawidjaja, R.; Myint, T.; Eilers, H. *Synthesis of Silver/Sio2/Eu:Lu2o3 Core-Shell Nanoparticles and Their Polymer Nanocomposites*, *Powder Technol.* **2011**, *210*, 157-166.

(18) Carretero-Palacios, S.; Calvo, M. E.; Míguez, H. *Absorption Enhancement in Organic-Inorganic Halide Perovskite Films with Embedded Plasmonic Gold Nanoparticles*, *J. Phys. Chem. C* **2015**, *119*, 18635-18640.

(19) Mali, S. S.; Shim, C. S.; Kim, H.; Patil, P. S.; Hong, C. K. *In Situ Processed Gold Nanoparticle-Embedded Tio2 Nanofibers Enabling Plasmonic Perovskite Solar Cells to Exceed 14% Conversion Efficiency*, *Nanoscale* **2016**, *8*, 2664-2677.

(20) Wang, J. Y.; Hsu, F. C.; Huang, J. Y.; Wang, L.; Chen, Y. F. *Bifunctional Polymer Nanocomposites as Hole-Transport Layers for Efficient Light Harvesting: Application to Perovskite Solar Cells*, *ACS Appl. Mater. Interfaces* **2015**, *7*, 27676-27684.

(21) Zhang, W.; Saliba, M.; Stranks, S. D.; Sun, Y.; Shi, X.; Wiesner, U.; Snaith, H. J. *Enhancement of Perovskite Based Solar Cells Employing Core-Shell Metal Nanoparticles*, *Nano Lett.* **2013**, *13*, 4505-4510.

(22) Marques-Hueso, J.; Abargues, R.; Valdes, J. L.; Martinez-Pastor, J. P. *Ag and Au/Dnq-Novolac Nanocomposites Patternable by Ultraviolet Lithography: A Fast Route to Plasmonic Sensor Microfabrication*, *J. Mater. Chem.* **2010**, *20*, 7436-7443.

(23) Gradess, R.; Abargues, R.; Habbou, A.; Canet-Ferrer, J.; Pedrueza, E.; Russell, A.; Valdes, J. L.; Martinez-Pastor, J. P. *Localized Surface Plasmon Resonance Sensor Based on Ag-Pva Nanocomposite Thin Films*, *J. Mater. Chem.* **2009**, *19*, 9233-9240.

(24) Abargues, R.; Abderrafi, K.; Pedrueza, E.; Gradess, R.; Marques-Hueso, J.; Valdes, J. L.; Martinez-Pastor, J. *Optical Properties of Different Polymer Thin Films Containing in Situ Synthesized Ag and Au Nanoparticles*, *New J. Chem.* **2009**, *33*, 1720-1725.

(25) Remita, H.; Lampre, I.; Mostafavi, M.; Balanzat, E.; Bouffard, S. *Comparative Study of Metal Clusters Induced in Aqueous Solutions by Gamma-Rays, Electron or C6+ Ion Beam Irradiation*, *Radiat. Phys. Chem.* **2005**, *72*, 575-586.

(26) Abargues, R.; Marques-Hueso, J.; Canet-Ferrer, J.; Pedrueza, E.; Valdes, J. L.; Jimenez, E.; Martinez-Pastor, J. P. *High-Resolution Electron-Beam Patternable Nanocomposite Containing Metal Nanoparticles for Plasmonics*, *Nanotechnology* **2008**, *19*.

(27) Mahapatra, S. K.; Bogle, K. A.; Dhole, S. D.; Bhoraskar, V. N. *Synthesis of Gold and Silver Nanoparticles by Electron Irradiation at 5-15 Kev Energy*, *Nanotechnology* **2007**, *18*.

(28) Boontongkong, Y.; Cohen, R. E. *Cavitated Block Copolymer Micellar Thin Films: Lateral Arrays of Open Nanoreactors*, *Macromolecules* **2002**, *35*, 3647-3652.

(29) Sohn, B. H.; Seo, B. H. *Fabrication of the Multilayered Nanostructure of Alternating Polymers and Gold Nanoparticles with Thin Films of Self-Assembling Diblock Copolymers*, *Chem. Mater.* **2001**, *13*, 1752-1757.

(30) Hashimoto, T.; Harada, M.; Sakamoto, N. *Incorporation of Metal Nanoparticles into Block Copolymer Nanodomains Via in-Situ Reduction of Metal Ions in Microdomain Space*, *Macromolecules* **1999**, *32*, 6867-6870.

(31) Wang, C.; Flynn, N. T.; Langer, R. *Controlled Structure and Properties of Thermoresponsive Nanoparticle-Hydrogel Composites*, *Adv. Mater.* **2004**, *16*, 1074-+.

(32) Mohan, Y. M.; Lee, K.; Premkumar, T.; Geckeler, K. E. *Hydrogel Networks as Nanoreactors: A Novel Approach to Silver Nanoparticles for Antibacterial Applications*, *Polymer* **2007**, *48*, 158-164.

(33) Karthikeyan, B.; Anija, M.; Philip, R. *In Situ Synthesis and Nonlinear Optical Properties of Au : Ag Nanocomposite Polymer Films*, *Appl. Phys. Lett.* **2006**, *88*.

(34) Porel, S.; Singh, S.; Radhakrishnan, T. P. *Polygonal Gold Nanoplates in a Polymer Matrix*, *Chem. Commun.* **2005**, 2387-2389.

(35) Porel, S.; Singh, S.; Harsha, S. S.; Rao, D. N.; Radhakrishnan, T. P. *Nanoparticle-Embedded Polymer: In Situ Synthesis, Free-Standing Films with Highly Monodisperse Silver Nanoparticles and Optical Limiting*, *Chem. Mater.* **2005**, *17*, 9-12.

(36) Mohan, Y. M.; Premkumar, T.; Lee, K.; Geckeler, K. E. *Fabrication of Silver Nanoparticles in Hydrogel Networks*, *Macromol. Rapid Commun.* **2006**, *27*, 1346-1354.

(37) Huang, H. Z.; Yuan, Q.; Yang, X. R. *Preparation and Characterization of Metal-Chitosan Nanocomposites*, *Colloids Surf. B. Biointerfaces* **2004**, *39*, 31-37.

(38) Saito, R.; Okamura, S.; Ishizu, K. *Introduction of Colloidal Silver into a Poly(2-Vinyl Pyridine) Microdomain of Microphase Separated Poly(Styrene-B-2-Vinyl Pyridine) Film*, *Polymer* **1992**, *33*, 1099-1101.

(39) Zhu, J. F.; Zhu, Y. J. *Microwave-Assisted One-Step Synthesis of Polyacrylamide - Metal (M) Ag, Pt, Cu) Nanocomposites in Ethylene Glycol*, *J. Phys. Chem. B* **2006**, *110*, 8593-8597.

(40) Li, S. M.; Jia, N.; Ma, M. G.; Zhang, Z.; Liu, Q. H.; Sun, R. C. *Cellulose-Silver Nanocomposites: Microwave-Assisted Synthesis, Characterization, Their Thermal Stability, and Antimicrobial Property*, *Carbohydr. Polym.* **2011**, *86*, 441-447.

(41) Zhang, Z. P.; Han, M. Y. *One-Step Preparation of Size-Selected and Well-Dispersed Silver Nanocrystals in Polyacrylonitrile by Simultaneous Reduction and Polymerization*, *J. Mater. Chem.* **2003**, *13*, 641-643.

(42) Takele, H.; Greve, H.; Pochstein, C.; Zaporojtchenko, V.; Faupel, F. *Plasmonic Properties of Ag Nanoclusters in Various Polymer Matrices*, *Nanotechnology* **2006**, *17*, 3499-3505.

(43) Schurmann, U.; Hartung, W.; Takele, H.; Zaporojtchenko, V.; Faupel, F. *Controlled Syntheses of Ag-Polytetrafluoroethylene Nanocomposite Thin Films by Co-Sputtering from Two Magnetron Sources*, *Nanotechnology* **2005**, *16*, 1078-1082.

(44) Schurmann, U.; Takele, H.; Zaporojtchenko, V.; Faupel, F. *Optical and Electrical Properties of Polymer Metal Nanocomposites Prepared by Magnetron Co-Sputtering*, *Thin Solid Films* **2006**, *515*, 801-804.

(45) Beyene, H. T.; Chakravadhanula, V. S. K.; Hanisch, C.; Elbahri, M.; Strunskus, T.; Zaporojtchenko, V.; Kienle, L.; Faupel, F. *Preparation and Plasmonic Properties of*

Polymer-Based Composites Containing Ag-Au Alloy Nanoparticles Produced by Vapor Phase Co-Deposition, *J. Mater. Sci.* **2010**, *45*, 5865-5871.

(46) Link, S.; El-Sayed, M. A. *Spectral Properties and Relaxation Dynamics of Surface Plasmon Electronic Oscillations in Gold and Silver Nanodots and Nanorods*, *J. Phys. Chem. B* **1999**, *103*, 8410-8426.

(47) Sonnichsen, C.; Franzl, T.; Wilk, T.; von Plessen, G.; Feldmann, J.; Wilson, O.; Mulvaney, P. *Drastic Reduction of Plasmon Damping in Gold Nanorods*, *Phys. Rev. Lett.* **2002**, *88*.

(48) Millstone, J. E.; Park, S.; Shuford, K. L.; Qin, L. D.; Schatz, G. C.; Mirkin, C. A. *Observation of a Quadrupole Plasmon Mode for a Colloidal Solution of Gold Nanoprisms*, *J. Am. Chem. Soc.* **2005**, *127*, 5312-5313.

(49) Graff, A.; Wagner, D.; Ditlbacher, H.; Kreibig, U. *Silver Nanowires*, *Eur. Phys. J. D* **2005**, *34*, 263-269.

(50) Jin, R. C.; Cao, Y. W.; Mirkin, C. A.; Kelly, K. L.; Schatz, G. C.; Zheng, J. G. *Photoinduced Conversion of Silver Nanospheres to Nanoprisms*, *Science* **2001**, *294*, 1901-1903.

(51) Sun, Y. G.; Xia, Y. N. *Shape-Controlled Synthesis of Gold and Silver Nanoparticles*, *Science* **2002**, *298*, 2176-2179.

(52) Jana, N. R.; Gearheart, L.; Murphy, C. J. *Wet Chemical Synthesis of Silver Nanorods and Nanowires of Controllable Aspect Ratio*, *Chem. Commun.* **2001**, 617-618.

(53) Jana, N. R.; Gearheart, L.; Murphy, C. J. *Wet Chemical Synthesis of High Aspect Ratio Cylindrical Gold Nanorods*, *J. Phys. Chem. B* **2001**, *105*, 4065-4067.

(54) Hore, M. J. A.; Composto, R. J. *Nanorod Self-Assembly for Tuning Optical Absorption*, *ACS Nano* **2010**, *4*, 6941-6949.

(55) Chiu, J. J.; Kim, B. J.; Kramer, E. J.; Pine, D. J. *Control of Nanoparticle Location in Block Copolymers*, *J. Am. Chem. Soc.* **2005**, *127*, 5036-5037.

(56) Mackay, M. E.; Tuteja, A.; Duxbury, P. M.; Hawker, C. J.; Van Horn, B.; Guan, Z. B.; Chen, G. H.; Krishnan, R. S. *General Strategies for Nanoparticle Dispersion*, *Science* **2006**, *311*, 1740-1743.

(57) Stewart, M. E.; Anderton, C. R.; Thompson, L. B.; Maria, J.; Gray, S. K.; Rogers, J. A.; Nuzzo, R. G. *Nanostructured Plasmonic Sensors*, *Chem. Rev.* **2008**, *108*, 494-521.

(58) Hore, M. J. A.; Frischknecht, A. L.; Composto, R. J. *Nanorod Assemblies in Polymer Films and Their Dispersion-Dependent Optical Properties*, *ACS Macro Lett.* **2012**, *1*, 115-121.

(59) Huang, H. Y.; Chen, W. F.; Kuo, P. L. *Self-Assembly of Gold Nanoparticles Induced by Poly(Oxypropylene)Diamines*, *J. Phys. Chem. B* **2005**, *109*, 24288-24294.

(60) Srivastava, S.; Frankamp, B. L.; Rotello, V. M. *Controlled Plasmon Resonance of Gold Nanoparticles Self-Assembled with Pamam Dendrimers*, *Chem. Mater.* **2005**, *17*, 487-490.

(61) Li, Q. F.; He, J. B.; Glogowski, E.; Li, X. F.; Wang, J.; Emrick, T.; Russell, T. P. *Responsive Assemblies: Gold Nanoparticles with Mixed Ligands in Microphase Separated Block Copolymers*, *Adv. Mater.* **2008**, *20*, 1462-+.

(62) Kim, B. J.; Bang, J.; Hawker, C. J.; Kramer, E. J. *Effect of Areal Chain Density on the Location of Polymer-Modified Gold Nanoparticles in a Block Copolymer Template*, *Macromolecules* **2006**, *39*, 4108-4114.

(63) Jang, S. G.; Khan, A.; Hawker, C. J.; Kramer, E. J. *Morphology Evolution of Ps-B-P2vp Diblock Copolymers Via Supramolecular Assembly of Hydroxylated Gold Nanoparticles*, *Macromolecules* **2012**, *45*, 1553-1561.

(64) Henzie, J.; Lee, M. H.; Odom, T. W. *Multiscale Patterning of Plasmonic Metamaterials*, *Nat. Nanotechnol.* **2007**, *2*, 549-554.

(65) Kauranen, M.; Zayats, A. V. *Nonlinear Plasmonics*, *Nat. Photonics* **2012**, *6*, 737-748.

(66) Dickson, W.; Wurtz, G. A.; Evans, P.; O'Connor, D.; Atkinson, R.; Pollard, R.; Zayats, A. V. *Dielectric-Loaded Plasmonic Nanoantenna Arrays: A Metamaterial with Tuneable Optical Properties*, *Phys. Rev. B* **2007**, *76*.

(67) Wurtz, G. A.; Pollard, R.; Hendren, W.; Wiederrecht, G. P.; Gosztola, D. J.; Podolskiy, V. A.; Zayats, A. V. *Designed Ultrafast Optical Nonlinearity in a Plasmonic Nanorod Metamaterial Enhanced by Nonlocality*, *Nat. Nanotechnol.* **2011**, *6*, 106-110.

(68) Le, F.; Brandl, D. W.; Urzhumov, Y. A.; Wang, H.; Kundu, J.; Halas, N. J.; Aizpurua, J.; Nordlander, P. *Metallic Nanoparticle Arrays: A Common Substrate for Both Surface-Enhanced Raman Scattering and Surface-Enhanced Infrared Absorption*, *ACS Nano* **2008**, *2*, 707-718.

(69) Adato, R.; Yanik, A. A.; Amsden, J. J.; Kaplan, D. L.; Omenetto, F. G.; Hong, M. K.; Erramilli, S.; Altug, H. *Ultra-Sensitive Vibrational Spectroscopy of Protein Monolayers with Plasmonic Nanoantenna Arrays*, *Proc. Natl. Acad. Sci. U. S. A.* **2009**, *106*, 19227-19232.

(70) Qin, L. D.; Zou, S. L.; Xue, C.; Atkinson, A.; Schatz, G. C.; Mirkin, C. A. *Designing, Fabricating, and Imaging Raman Hot Spots*, *Proc. Natl. Acad. Sci. U. S. A.* **2006**, *103*, 13300-13303.

(71) Mirin, N. A.; Bao, K.; Nordlander, P. *Fano Resonances in Plasmonic Nanoparticle Aggregates*, *J. Phys. Chem. A* **2009**, *113*, 4028-4034.

(72) Fan, J. A.; Wu, C. H.; Bao, K.; Bao, J. M.; Bardhan, R.; Halas, N. J.; Manoharan, V. N.; Nordlander, P.; Shvets, G.; Capasso, F. *Self-Assembled Plasmonic Nanoparticle Clusters*, *Science* **2010**, *328*, 1135-1138.

(73) Hentschel, M.; Saliba, M.; Vogelgesang, R.; Giessen, H.; Alivisatos, A. P.; Liu, N. *Transition from Isolated to Collective Modes in Plasmonic Oligomers*, *Nano Lett.* **2010**, *10*, 2721-2726.

(74) Bao, K.; Mirin, N. A.; Nordlander, P. *Fano Resonances in Planar Silver Nanosphere Clusters*, *Appl. Phys. A Mater. Sci. Process.* **2010**, *100*, 333-339.

(75) Kao, J.; Bai, P.; Chuang, V. P.; Jiang, Z.; Ercius, P.; Xu, T. *Nanoparticle Assemblies in Thin Films of Supramolecular Nanocomposites*, *Nano Lett.* **2012**, *12*, 2610-2618.

(76) Zhao, Y.; Thorkelsson, K.; Mastroianni, A. J.; Schilling, T.; Luther, J. M.; Rancatore, B. J.; Matsunaga, K.; Jinnai, H.; Wu, Y.; Poulsen, D.; Frechet, J. M. J.; Alivisatos, A. P.; Xu, T. *Small-Molecule-Directed Nanoparticle Assembly Towards Stimuli-Responsive Nanocomposites*, *Nat. Mater.* **2009**, *8*, 979-985.

(77) Thorkelsson, K.; Nelson, J. H.; Alivisatos, A. P.; Xu, T. *End-to-End Alignrnent of Nanorods in Thin Films*, *Nano Lett.* **2013**, *13*, 4908-4913.

(78) Son, J. G.; Bae, W. K.; Kang, H. M.; Nealey, P. F.; Char, K. *Placement Control of Nanomaterial Arrays on the Surface-Reconstructed Block Copolymer Thin Films*, *ACS Nano* **2009**, *3*, 3927-3934.

(79) Shukla, S.; Kim, K. T.; Baev, A.; Yoon, Y. K.; Litchinitser, N. M.; Prasad, P. N. *Fabrication and Characterization of Gold-Polymer Nanocomposite Plasmonic Nanoarrays in a Porous Alumina Template*, *ACS Nano* **2010**, *4*, 2249-2255.

(80) Ng, K. C.; Udagedara, I. B.; Rukhlenko, I. D.; Chen, Y.; Tang, Y.; Premaratne, M.; Cheng, W. L. *Free-Standing Plasmonic-Nanorod Super Lattice Sheets*, *ACS Nano* **2012**, *6*, 925-934.

(81) Querejeta-Fernandez, A.; Chauve, G.; Methot, M.; Bouchard, J.; Kumacheva, E. *Chiral Plasmonic Films Formed by Gold Nanorods and Cellulose Nanocrystals*, *J. Am. Chem. Soc.* **2014**, *136*, 4788-4793.

(82) Querejeta-Fernandez, A.; Kopera, B.; Prado, K. S.; Klinkova, A.; Methot, M.; Chauve, G.; Bouchard, J.; Helmy, A. S.; Kumacheva, E. *Circular Dichroism of Chiral Nematic Films of Cellulose Nanocrystals Loaded with Plasmonic Nanoparticles*, *ACS Nano* **2015**, *9*, 10377-10385.

(83) Xu, W.; Ling, X.; Xiao, J.; Dresselhaus, M. S.; Kong, J.; Xu, H.; Liu, Z.; Zhang, J. *Surface Enhanced Raman Spectroscopy on a Flat Graphene Surface*, *Proc. Natl. Acad. Sci.* **2012**, *109*, 9281-9286.

(84) Chen, X. C.; Green, P. F. *Control of Morphology and Its Effects on the Optical Properties of Polymer Nanocomposites*, *Langmuir* **2010**, *26*, 3659-3665.

(85) Slaughter, L. S.; Willingham, B. A.; Chang, W. S.; Chester, M. H.; Ogden, N.; Link, S. *Toward Plasmonic Polymers*, *Nano Lett.* **2012**, *12*, 3967-3972.

(86) Kang, Y. J.; Erickson, K. J.; Taton, T. A. *Plasmonic Nanoparticle Chains Via a Morphological, Sphere-to-String Transition*, *J. Am. Chem. Soc.* **2005**, *127*, 13800-13801.

(87) Choi, J. H.; Adams, S. M.; Ragan, R. *Design of a Versatile Chemical Assembly Method for Patterning Colloidal Nanoparticles*, *Nanotechnology* **2009**, *20*.

(88) Sardar, R.; Shumaker-Parry, J. S. *Asymmetrically Functionalized Gold Nanoparticles Organized in One-Dimensional Chains*, *Nano Lett.* **2008**, *8*, 731-736.

(89) DeVries, G. A.; Brunnbauer, M.; Hu, Y.; Jackson, A. M.; Long, B.; Neltner, B. T.; Uzun, O.; Wunsch, B. H.; Stellacci, F. *Divalent Metal Nanoparticles*, *Science* **2007**, *315*, 358-361.

(90) Liu, K.; Ahmed, A.; Chung, S. Y.; Sugikawa, K.; Wu, G. X.; Nie, Z. H.; Gordon, R.; Kumacheva, E. *In Situ Plasmonic Counter for Polymerization of Chains of Gold Nanorods in Solution*, *ACS Nano* **2013**, *7*, 5901-5910.

(91) Liu, K.; Nie, Z. H.; Zhao, N. N.; Li, W.; Rubinstein, M.; Kumacheva, E. *Step-Growth Polymerization of Inorganic Nanoparticles*, *Science* **2010**, *329*, 197-200.

(92) Lukach, A.; Liu, K.; Therien-Aubin, H.; Kumacheva, E. *Controlling the Degree of Polymerization, Bond Lengths, and Bond Angles of Plasmonic Polymers*, *J. Am. Chem. Soc.* **2012**, *134*, 18853-18859.

(93) Liu, K.; Lukach, A.; Sugikawa, K.; Chung, S.; Vickery, J.; Therien-Aubin, H.; Yang, B.; Rubinstein, M.; Kumacheva, E. *Copolymerization of Metal Nanoparticles: A Route to Colloidal Plasmonic Copolymers*, *Angew. Chem. Int. Ed.* **2014**, *53*, 2648-2653.

(94) Fava, D.; Nie, Z.; Winnik, M. A.; Kumacheva, E. *Evolution of Self-Assembled Structures of Polymer-Terminated Gold Nanorods in Selective Solvents*, *Adv. Mater.* **2008**, *20*, 4318-4322.

(95) Xia, Y.; Rogers, J. A.; Paul, K. E.; Whitesides, G. M. *Unconventional Methods for Fabricating and Patterning Nanostructures*, *Chem. Rev.* **1999**, *99*, 1823-1848.

(96) Israelachvili, J. N. *Intermolecular and Surface Forces*; Academic Press, 1992.

(97) Nikoobakht, B.; Wang, Z. L.; El-Sayed, M. A. *Self-Assembly of Gold Nanorods*, *J. Phys. Chem. B* **2000**, *104*, 8635-8640.

(98) Chen, M.; Kim, J.; Liu, J. P.; Fan, H.; Sun, S. *Synthesis of Fept Nanocubes and Their Oriented Self-Assembly*, *J. Am. Chem. Soc.* **2006**, *128*, 7132-7133.

(99) Ren, J.; Tilley, R. D. *Preparation, Self-Assembly, and Mechanistic Study of Highly Monodispersed Nanocubes*, *J. Am. Chem. Soc.* **2007**, *129*, 3287-3291.

(100) Nie, Z. H.; Fava, D.; Rubinstein, M.; Kumacheva, E. *"Supramolecular" Assembly of Gold Nanorods End-Terminated with Polymer "Pom-Poms": Effect of Pom-Pom Structure on the Association Modes*, *J. Am. Chem. Soc.* **2008**, *130*, 3683-3689.

(101) Nie, Z. H.; Fava, D.; Kumacheva, E.; Zou, S.; Walker, G. C.; Rubinstein, M. *Self-Assembly of Metal-Polymer Analogues of Amphiphilic Triblock Copolymers*, *Nat. Mater.* **2007**, *6*, 609-614.

(102) Gurunatha, K. L.; Marvi, S.; Arya, G.; Tao, A. R. *Computationally Guided Assembly of Oriented Nanocubes by Modulating Grafted Polymer–Surface Interactions*, *Nano Lett.* **2015**, *15*, 7377-7382.

(103) Gao, B.; Arya, G.; Tao, A. R. *Self-Orienting Nanocubes for the Assembly of Plasmonic Nanojunctions*, *Nature Nanotechnology* **2012**, *7*, 433-437.

(104) Gao, B.; Alvi, Y.; Rosen, D.; Lav, M.; Tao, A. R. *Designer Nanojunctions: Orienting Shaped Nanoparticles within Polymer Thin-Film Nanocomposites*, *Chem. Commun.* **2013**, *49*, 4382-4384.

(105) Rosen, D. A.; Tao, A. R. *Modeling the Optical Properties of Bowtie Antenna Generated by Self-Assembled Ag Triangular Nanoprisms*, *ACS Appl. Mater. Interfaces* **2014**, *6*, 4134-4142.

(106) Dill, T. J.; Rozin, M. J.; Brown, E. R.; Palani, S.; Tao, A. R. *Investigating the Effect of Ag Nanocube Polydispersity on Gap-Mode Sers Enhancement Factors*, *Analyst.* **2016**, *141*, 3916-3924.

(107) Pal, S.; Deng, Z.; Ding, B.; Yan, H.; Liu, Y. *DNA-Origami-Directed Self-Assembly of Discrete Silver-Nanoparticle Architectures*, *Angew. Chem. Int. Ed.* **2010**, *49*, 2700-2704.

(108) Kuzyk, A.; Schreiber, R.; Fan, Z.; Pardatscher, G.; Roller, E.-M.; Högele, A.; Simmel, F. C.; Govorov, A. O.; Liedl, T. *DNA-Based Self-Assembly of Chiral Plasmonic Nanostructures with Tailored Optical Response*, *Nature* **2012**, *483*, 311-314.

(109) Schreiber, R.; Do, J.; Roller, E.-m.; Zhang, T.; Schüller, V. J.; Nickels, P. C.; Feldmann, J.; Liedl, T. *Hierarchical Assembly of Metal Nanoparticles, Quantum Dots and Organic Dyes Using DNA Origami Scaffolds*, *Nat. Nanotechnol.* **2014**, *9*, 74-78.

(110) Zhang, Y.; Lu, F.; Yager, K. G.; van der Lelie, D.; Gang, O. *A General Strategy for the DNA-Mediated Self-Assembly of Functional Nanoparticles into Heterogeneous Systems*, *Nat. Nanotechnol.* **2013**, *8*, 865-872.

(111) Sun, L.; Lin, H.; Park, D. J.; Bourgeois, M. R.; Ross, M. B.; Ku, J. C.; Schatz, G. C.; Mirkin, C. A. *Polarization-Dependent Optical Response in Anisotropic Nanoparticle-DNA Superlattices*, *Nano Lett.* **2017**, *17*, 2313-2318.

(112) Morfa, A. J.; Rowlenthomas, K. L.; Iii, H. R.; Romero, M. J.; Lagemaat, J. V. D.; Rowlen, K. L. *Plasmon-Enhanced Solar Energy Conversion in Organic Bulk Heterojunction Photovoltaics*, *Appl. Phys. Lett.* **2008**, *92*, 013504-013504.

(113) Ou, J.-Y.; Plum, E.; Zhang, J.; Zheludev, N. I. *An Electromechanically Reconfigurable Plasmonic Metamaterial Operating in the near-Infrared*, *Nat. Nanotechnol.* **2013**, *8*, 252-255.

(114) Aksu, S.; Huang, M.; Artar, A.; Yanik, A. A.; Selvarasah, S.; Dokmeci, M. R.; Altug, H. *Flexible Plasmonics: Flexible Plasmonics on Unconventional and Nonplanar Substrates (Adv. Mater. 38/2011)*, *Adv. Mater.* **2011**, *23*, 4421-4421.

(115) Zhu, J.; Li, J.-J.; Yuan, L.; Zhao, J.-W. *Optimization of Three-Layered Au–Ag Bimetallic Nanoshells for Triple-Bands Surface Plasmon Resonance*, *J. Phys. Chem. C* **2012**, *116*, 11734-11740.

(116) Minnai, C.; Milani, P. *Metal-Polymer Nanocomposite with Stable Plasmonic Tuning under Cyclic Strain Conditions*, *Appl. Phys. Lett.* **2015**, *107*, 073106.

(117) Malek, S. C.; Ee, H.-S.; Agarwal, R. *Strain Multiplexed Metasurface Holograms on a Stretchable Substrate*, *Nano Lett.* **2017**, *17*, 3641-3645.

(118) Heskins, M.; Guillet, J. E. *Solution Properties of Poly (N-Isopropylacrylamide)*, *J. Macromol. Sci. Pure Appl. Chem.* **1968**, *2*, 1441-1455.

(119) Zhu, M.-Q.; Wang, L.-Q.; Exarhos, G. J.; Li, A. D. Q. *Thermosensitive Gold Nanoparticles*, *J. Am. Chem. Soc.* **2004**, *126*, 2656-2657.

(120) Ding, T.; Valev, V. K.; Salmon, A. R.; Forman, C. J.; Smoukov, S. K.; Scherman, O. A.; Frenkel, D.; Baumberg, J. J. *Light-Induced Actuating Nanotransducers*, *Proc. Natl. Acad. Sci.* **2016**, *113*, 5503-5507.

(121) Roiter, Y.; Minko, I.; Nykypanchuk, D.; Tokarev, I.; Minko, S. *Mechanism of Nanoparticle Actuation by Responsive Polymer Brushes: From Reconfigurable Composite Surfaces to Plasmonic Effects*, *Nanoscale* **2012**, *4*, 284-292.

(122) Kim, Y.; Yeom, B.; Arteaga, O.; Jo Yoo, S.; Lee, S.-G.; Kim, J.-G.; Kotov, N. A. *Reconfigurable Chiroptical Nanocomposites with Chirality Transfer from the Macro- to the Nanoscale*, *Nat. Mater.* **2016**, *15*, 461-468.

(123) Zhang, J.; Santos, P. J.; Gabrys, P. A.; Lee, S.; Liu, C.; Macfarlane, R. J. *Self-Assembling Nanocomposite Tectons*, *J. Am. Chem. Soc.* **2016**, *138*, 16228-16231.

(124) Liu, Q.; Cui, Y.; Gardner, D.; Li, X.; He, S.; Smalyukh, I. I. *Self-Alignment of Plasmonic Gold Nanorods in Reconfigurable Anisotropic Fluids for Tunable Bulk Metamaterial Applications*, *Nano Lett.* **2010**, *10*, 1347-1353.

(125) Zhang, Y.; Liu, Q.; Mundoor, H.; Yuan, Y.; Smalyukh, I. I. *Metal Nanoparticle Dispersion, Alignment, and Assembly in Nematic Liquid Crystals for Applications in Switchable Plasmonic Color Filters and E-Polarizers*, *ACS Nano* **2015**, *9*, 3097-3108.

(126) Wojcik, M. M.; Gora, M.; Mieczkowski, J.; Romiszewski, J.; Gorecka, E.; Pociecha, D. *Temperature-Controlled Liquid Crystalline Polymorphism of Gold Nanoparticles*, *Soft Mater.* **2011**, *7*, 10561-10564.

(127) Wolska, J. M.; Pociecha, D.; Mieczkowski, J.; Gorecka, E. *Control of Sample Alignment Mode for Hybrid Lamellar Systems Based on Gold Nanoparticles*, *Chem. Commun.* **2014**, *50*, 7975-7978.

(128) Lewandowski, W.; Fruhnert, M.; Mieczkowski, J.; Rockstuhl, C.; Górecka, E. *Dynamically Self-Assembled Silver Nanoparticles as a Thermally Tunable Metamaterial*, *Nat. Commun.* **2015**, *6*, 6590.

(129) Rožič, B.; Fresnais, J.; Molinaro, C.; Calixte, J.; Umadevi, S.; Lau-Truong, S.; Felidj, N.; Kraus, T.; Charra, F.; Dupuis, V.; Hegmann, T.; Fiorini-Debuisschert, C.; Gallas, B.; Lacaze, E. *Oriented Gold Nanorods and Gold Nanorod Chains within Smectic Liquid Crystal Topological Defects*, *ACS Nano* **2017**, *11*, 6728-6738.

(130) Pletsch, H.; Tebbe, M.; Dulle, M.; Förster, B.; Fery, A.; Förster, S.; Greiner, A.; Agarwal, S. *Reversible Gold Nanorod Alignment in Mechano-Responsive Elastomers*, *Polymer* **2015**, *66*, 167-172.

(131) Gao, L.; Zhang, Y.; Zhang, H.; Doshay, S.; Xie, X.; Luo, H.; Shah, D.; Shi, Y.; Xu, S.; Fang, H.; Fan, J. A.; Nordlander, P.; Huang, Y.; Rogers, J. A. *Optics and Nonlinear*

Buckling Mechanics in Large-Area, Highly Stretchable Arrays of Plasmonic Nanostructures, *ACS Nano* **2015**, *9*, 5968-5975.

(132) Wilson, O.; Wilson, G. J.; Mulvaney, P. *Laser Writing in Polarized Silver Nanorod Films*, *Adv. Mater.* **2002**, *14*, 1000-1004.

(133) Link, S.; Burda, C.; Mohamed, M. B.; Nikoobakht, B.; El-Sayed, M. A. *Laser Photothermal Melting and Fragmentation of Gold Nanorods: Energy and Laser Pulse-Width Dependence*, *J. Phys. Chem. A* **1999**, *103*, 1165-1170.

(134) Montelongo, Y.; Yetisen, A. K.; Butt, H.; Yun, S.-H. *Reconfigurable Optical Assembly of Nanostructures*, *Nat. Commun.* **2016**, *7*, 12002.

(135) Ledin, P. A.; Jeon, J.-W.; Geldmeier, J. A.; Ponder, J. F.; Mahmoud, M. A.; El-Sayed, M.; Reynolds, J. R.; Tsukruk, V. V. *Design of Hybrid Electrochromic Materials with Large Electrical Modulation of Plasmonic Resonances*, *ACS Appl. Mater. Interfaces* **2016**, *8*, 13064-13075.

(136) Ledin, P. A.; Russell, M.; Geldmeier, J. A.; Tkachenko, I. M.; Mahmoud, M. A.; Shevchenko, V.; El-Sayed, M. A.; Tsukruk, V. V. *Light-Responsive Plasmonic Arrays Consisting of Silver Nanocubes and a Photoisomerizable Matrix*, *ACS Appl. Mater. Interfaces* **2015**, *7*, 4902-4912.

(137) Yu, N.; Capasso, F. *Flat Optics with Designer Metasurfaces*, *Nat Mater* **2014**, *13*, 139-150.

(138) Subramaniam, A. B.; Abkarian, M.; Mahadevan, L.; Stone, H. A. *Mechanics of Interfacial Composite Materials*, *Langmuir* **2006**, *22*, 10204-10208.

(139) Sherry, L. J.; Chang, S.-H.; Schatz, G. C.; Van Duyne, R. P.; Wiley, B. J.; Xia, Y. *Localized Surface Plasmon Resonance Spectroscopy of Single Silver Nanocubes*, *Nano Lett.* **2005**, *5*, 2034-2038.

(140) Zhang, Y. A.; Stokes, N.; Jia, B.; Fan, S. H.; Gu, M. *Towards Ultra-Thin Plasmonic Silicon Wafer Solar Cells with Minimized Efficiency Loss*, *Sci. Rep.* **2014**, *4*.

(141) Nourolahi, H.; Behjat, A.; Hosseini Zarch, S. M. M.; Bolorizadeh, M. A. *Silver Nanoparticle Plasmonic Effects on Hole-Transport Material-Free Mesoporous Heterojunction Perovskite Solar Cells*, *Solar Energy* **2016**, *139*, 475-483.

(142) Wu, J. L.; Chen, F. C.; Hsiao, Y. S.; Chien, F. C.; Chen, P.; Kuo, C. H.; Huang, M. H.; Hsu, C. S. *Surface Plasmonic Effects of Metallic Nanoparticles on the Performance of Polymer Bulk Heterojunction Solar Cells*, *ACS Nano* **2011**, *5*, 959-967.

(143) Catchpole, K. R.; Polman, a. *Plasmonic Solar Cells*, *Opt. Express* **2008**, *16*, 21793-21800.

(144) Beck, F. J.; Polman, A.; Catchpole, K. R. *Tunable Light Trapping for Solar Cells Using Localized Surface Plasmons*, *J. Appl. Phys.* **2009**, *105*, 1143101-1143107.

(145) Zhang, N.; Liu, K.; Song, H.; Liu, Z.; Ji, D.; Zeng, X.; Jiang, S.; Gan, Q. *Refractive Index Engineering of Metal-Dielectric Nanocomposite Thin Films for Optical Super Absorber*, *Appl. Phys. Lett.* **2014**, *104*, 203112.

(146) Akimov, Y. a.; Koh, W. S.; Ostrikov, K. *Enhancement of Optical Absorption in Thin-Film Solar Cells through the Excitation of Higher-Order Nanoparticle Plasmon Modes*, *Opt. Express* **2009**, *17*, 10195-10205.

(147) Ferry, V. E.; Verschuuren, M. A.; Li, H. B. T.; Verhagen, E.; Walters, R. J.; Schropp, R. E. I.; Atwater, H. A.; Polman, A. *Light Trapping in Ultrathin Plasmonic Solar Cells*, *Opt. Express* **2010**, *18*, A237--A245.

(148) Pastorelli, F.; Bidault, S.; Martorell, J.; Bonod, N. *Self-Assembled Plasmonic Oligomers for Organic Photovoltaics*, *Adv. Opt. Mater.* **2014**, *2*, 171-175.

(149) Chen, F. C.; Wu, J. L.; Lee, C. L.; Hong, Y.; Kuo, C. H.; Huang, M. H. *Plasmonic-Enhanced Polymer Photovoltaic Devices Incorporating Solution-Processable Metal Nanoparticles*, *Appl. Phys. Lett.* **2009**, *95*, 2007-2010.

(150) Kao, C.-S.; Chen, F.-C.; Liao, C.-W.; Huang, M. H.; Hsu, C.-S. *Plasmonic-Enhanced Performance for Polymer Solar Cells Prepared with Inverted Structures*, *Appl. Phys. Lett.* **2012**, *101*, 193902-193902.

(151) Jang, Y. H.; Jang, Y. J.; Kim, S.; Quan, L. N.; Chung, K.; Kim, D. H. *Plasmonic Solar Cells: From Rational Design to Mechanism Overview*, *Chem. Rev.* **2016**, *116*, 14982-15034.

(152) Clavero, C. *Plasmon-Induced Hot-Electron Generation at Nanoparticle/Metal-Oxide Interfaces for Photovoltaic and Photocatalytic Devices*, *Nat. Photonics* **2014**, *8*, 95-103.

(153) Ohko, Y.; Tatsuma, T.; Fujii, T.; Naoi, K.; Niwa, C.; Kubota, Y.; Fujishima, A. *Multicolour Photochromism of Tio2 Films Loaded with Silver Nanoparticles*, *Nat. Mater.* **2003**, *2*, 29-31.

(154) Yang, J.; You, J.; Chen, C. C.; Hsu, W. C.; Tan, H. R.; Zhang, X. W.; Hong, Z.; Yang, Y. *Plasmonic Polymer Tandem Solar Cell*, *ACS Nano* **2011**, *5*, 6210-6217.

(155) Lu, L.; Luo, Z.; Xu, T.; Yu, L. *Cooperative Plasmonic Effect of Ag and Au Nanoparticles on Enhancing Performance of Polymer Solar Cells*, *Nano Lett.* **2013**, *13*, 59-64.

(156) Hsiao, Y.-s.; Charan, S.; Wu, F.-y.; Chien, F.-c.; Chu, C.-w.; Chen, P.; Chen, F.-c. *Improving the Light Trapping E Ffi Ciency of Plasmonic Polymer Solar Cells through Photon Management*, *J. Phys. Chem. C* **2012**, *116*, 20731-20737.

(157) Yang, X.; Chueh, C. C.; Li, C. Z.; Yip, H. L.; Yin, P.; Chen, H.; Chen, W. C.; Jen, A. K. Y. *High-Efficiency Polymer Solar Cells Achieved by Doping Plasmonic Metallic Nanoparticles into Dual Charge Selecting Interfacial Layers to Enhance Light Trapping*, *Adv. Energy Mater.* **2013**, *3*, 666-673.

(158) Baek, S.-W.; Noh, J.; Lee, C.-H.; Kim, B.; Seo, M.-K.; Lee, J.-Y. *Plasmonic Forward Scattering Effect in Organic Solar Cells: A Powerful Optical Engineering Method*, *Sci. Rep.* **2013**, *3*, 1726-1726.

(159) Yao, K.; Salvador, M.; Chueh, C.-C.; Xin, X.-K.; Xu, Y.-X.; DeQuilettes, D. W.; Hu, T.; Chen, Y.; Ginger, D. S.; Jen, A. K. Y. *A General Route to Enhance Polymer Solar Cell Performance Using Plasmonic Nanoprisms*, *Adv. Energy Mater.* **2014**, *4*, 1400206-1400206.

(160) Lu, Z.; Pan, X.; Ma, Y.; Li, Y.; Zheng, L.; Zhang, D.; Xu, Q.; Chen, Z.; Wang, S.; Qu, B.; Liu, F.; Huang, Y.; Xiao, L.; Gong, Q. *Plasmonic-Enhanced Perovskite Solar Cells Using Alloy Popcorn Nanoparticles*, *J. Mater. Chem.* **2015**, *5*, 11175-11179.

(161) Hong, W.; Bai, H.; Xu, Y.; Yao, Z.; Gu, Z.; Shi, G. *Preparation of Gold Nanoparticle/Graphene Composites with Controlled Weight Contents and Their Application in Biosensors*, *J. Phys. Chem. C* **2010**, *114*, 1822-1826.

(162) Zhang, H.; Fan, X.; Quan, X.; Chen, S.; Yu, H. *Graphene Sheets Grafted Ag@Agcl Hybrid with Enhanced Plasmonic Photocatalytic Activity under Visible Light*, *Environ. Sci. Technol.* **2011**, *45*, 5731-5736.

(163) Liu, Y.; Cheng, R.; Liao, L.; Zhou, H.; Bai, J.; Liu, G.; Liu, L.; Huang, Y.; Duan, X. *Plasmon Resonance Enhanced Multicolour Photodetection by Graphene*, *Nat. Commun.* **2011**, *2*, 579.

(164) Yang, X.; Liu, W.; Xiong, M.; Zhang, Y.; Liang, T.; Yang, J.; Xu, M.; Ye, J.; Chen, H. *Au Nanoparticles on Ultrathin Mos2 Sheets for Plasmonic Organic Solar Cells*, *J. Mater. Chem. A* **2014**, *2*, 14798-14806.

(165) Xu, Q.; Jiang, D.; Wang, T.; Meng, S.; Chen, M. *Ag Nanoparticle-Decorated Cos Nanosheet Nanocomposites: A High-Performance Material for Multifunctional Applications in Photocatalysis and Supercapacitors*, *RSC Adv.* **2016**, *6*, 55039-55045.

(166) Sobhani, A.; Lauchner, A.; Najmaei, S.; Ayala-Orozco, C.; Wen, F.; Lou, J.; Halas, N. J. *Enhancing the Photocurrent and Photoluminescence of Single Crystal Monolayer Mos2 with Resonant Plasmonic Nanoshells*, *Appl. Phys. Lett.* **2014**, *104*, 031112.

(167) Chuang, M.-K.; Yang, S.-S.; Chen, F.-C. *Metal Nanoparticle-Decorated Two-Dimensional Molybdenum Sulfide for Plasmonic-Enhanced Polymer Photovoltaic Devices*, *Materials* **2015**, *8*, 5414-5425.

(168) Marin, B. C.; Liu, J.; Aklile, E.; Urbina, A. D.; Chiang, A. S. C.; Lawrence, N.; Chen, S.; Lipomi, D. J. *Sers-Enhanced Piezoplasmonic Graphene Composite for Biological and Structural Strain Mapping*, *Nanoscale* **2017**.

(169) Xia, Z.; Li, P.; Wang, Y.; Song, T.; Zhang, Q.; Sun, B. *Solution-Processed Gold Nanorods Integrated with Graphene for near-Infrared Photodetection Via Hot Carrier Injection*, *ACS Appl. Mater. Interfaces* **2015**, *7*, 24136-24141.

(170) Landy, N. I.; Sajuyigbe, S.; Mock, J. J.; Smith, D. R.; Padilla, W. J. *Perfect Metamaterial Absorber*, *Phys. Rev. Lett.* **2008**, *100*, 2074021-2074024.

(171) Liu, N.; Mesch, M.; Weiss, T.; Hentschel, M.; Giessen, H. *Infrared Perfect Absorber and Its Application as Plasmonic Sensor*, *Nano Lett.* **2010**, *10*, 2342-2348.

(172) Zhang, B.; Zhao, Y.; Hao, Q.; Kiraly, B.; Khoo, I.-C.; Chen, S.; Huang, T. J. *Polarization-Independent Dual-Band Infrared Perfect Absorber Based on a Metal-Dielectric-Metal Elliptical Nanodisk Array*, *Opt. Express* **2011**, *19*, 15221-15221.

(173) Moreau, A.; Ciracı, C.; Mock, J. J.; Hill, R. T.; Wang, Q.; Wiley, B. J.; Chilkoti, A.; Smith, D. R. *Controlled-Reflectance Surfaces with Film-Coupled Colloidal Nanoantennas*, *Nature* **2012**, *492*, 86-90.

(174) Lassiter, J. B.; McGuire, F.; Mock, J. J.; Ciracì, C.; Hill, R. T.; Wiley, B. J.; Chilkoti, A.; Smith, D. R. *Plasmonic Waveguide Modes of Film-Coupled Metallic Nanocubes*, *Nano Lett.* **2013**, *13*, 5866-5872.

(175) Akselrod, G. M.; Huang, J.; Hoang, T. B.; Bowen, P. T.; Su, L.; Smith, D. R.; Mikkelsen, M. H. *Large-Area Metasurface Perfect Absorbers from Visible to near-Infrared*, *Adv. Mater.* **2015**, *27*, 8028-8034.

(176) Rozin, M. J.; Rosen, D. A.; Dill, T. J.; Tao, A. R. *Colloidal Metasurfaces Displaying near-Ideal and Tunable Light Absorbance in the Infrared*, *Nat. Commun.* **2015**, *6*, 7325-7325.

(177) Liu, Z.; Liu, X.; Huang, S.; Pan, P.; Chen, J.; Liu, G.; Gu, G. *Automatically Acquired Broadband Plasmonic-Metamaterial Black Absorber During the Metallic Film-Formation*, *ACS Appl. Mater. Interfaces* **2015**, *7*, 4962-4968.

(178) Hedayati, M. K.; Javaherirahim, M.; Mozooni, B.; Abdelaziz, R.; Tavassolizadeh, A.; Chakravadhanula, V. S. K.; Zaporojtchenko, V.; Strunkus, T.; Faupel, F.; Elbahri, M. *Design of a Perfect Black Absorber at Visible Frequencies Using Plasmonic Metamaterials*, *Adv. Mater.* **2011**, *23*, 5410-5414.

(179) Lin, Q. Y.; Li, Z.; Brown, K. A.; O'Brien, M. N.; Ross, M. B.; Zhou, Y.; Butun, S.; Chen, P. C.; Schatz, G. C.; Dravid, V. P.; Aydin, K.; Mirkin, C. A. *Strong Coupling between Plasmonic Gap Modes and Photonic Lattice Modes in DNA-Assembled Gold Nanocube Arrays*, *Nano Lett.* **2015**, *15*, 4699-4703.

(180) Zhang, N.; Dong, Z.; Ji, D.; Song, H.; Zeng, X.; Liu, Z.; Jiang, S.; Xu, Y.; Bernussi, A.; Li, W.; Gan, Q. *Reversibly Tunable Coupled and Decoupled Super Absorbing Structures*, *Appl. Phys. Lett.* **2016**, *108*, 0911051-0911055.

(181) Zhou, L.; Tan, Y.; Ji, D.; Zhu, B.; Zhang, P.; Xu, J.; Gan, Q.; Yu, Z.; Zhu, J. *Self-Assembly of Highly Efficient, Broadband Plasmonic Absorbers for Solar Steam Generation*, *Sci. Adv* **2016**, *2*, e1501227-e1501227.

(182) Elbahri, M.; Hedayati, M. K.; Kiran Chakravadhanula, V. S.; Jamali, M.; Strunkus, T.; Zaporojtchenko, V.; Faupel, F. *An Omnidirectional Transparent Conducting-Metal-Based Plasmonic Nanocomposite*, *Adv. Mater.* **2011**, *23*, 1993-1997.

(183) Hedayati, M. K.; Faupel, F.; Elbahri, M. *Tunable Broadband Plasmonic Perfect Absorber at Visible Frequency*, *Appl. Phys. A Mater. Sci. Process.* **2012**, *109*, 769-773.

(184) Hedayati, M. K.; Zillohu, A. U.; Strunskus, T.; Faupel, F.; Elbahri, M. *Plasmonic Tunable Metamaterial Absorber as Ultraviolet Protection Film*, *Appl. Phys. Lett.* **2014**, *104*, 0411031-0411035.

(185) Hedayati, M. K.; Javaheri, M.; Zillohu, A. U.; El-Khozondar, H. J.; Bawa'aneh, M. S.; Lavrinenko, A.; Faupel, F.; Elbahri, M. *Photo-Driven Super Absorber as an Active Metamaterial with a Tunable Molecular-Plasmonic Coupling*, *Adv. Opt. Mater.* **2014**, *2*, 705-710.

(186) Tan, F.; Wang, N.; Lei, D. Y.; Yu, W.; Zhang, X. *Plasmonic Black Absorbers for Enhanced Photocurrent of Visible-Light Photocatalysis*, *Adv. Opt. Mater.* **2017**, *5*, 1600399-1600399.

(187) Stewart, J. W.; Akselrod, G.; Smith, D. R.; Mikkelsen, M. H. *Toward Multispectral Imaging with Colloidal Metasurface Pixels*, *Adv. Mater.* **2017**, *29*, 1602971-1602977.

(188) Liu, X.; Tyler, T.; Starr, T.; Starr, A. F.; Jokerst, N. M.; Padilla, W. J. *Taming the Blackbody with Infrared Metamaterials as Selective Thermal Emitters*, *Phys. Rev. Lett.* **2011**, *107*, 4-7.

(189) Rose, A.; Hoang, T. B.; McGuire, F.; Mock, J. J.; Cirac, C.; Smith, D. R.; Mikkelsen, M. H. *Control of Radiative Processes Using Tunable Plasmonic Nanopatch Antennas*, *Nano Lett.* **2014**, *14*, 4797-4802.

(190) Akselrod, G. M.; Argyropoulos, C.; Hoang, T. B.; Ciracì, C.; Fang, C.; Huang, J.; Smith, D. R.; Mikkelsen, M. H. *Probing the Mechanisms of Large Purcell Enhancement in Plasmonic Nanoantennas*, *Nat. Photonics* **2014**, *8*, 835-840.

(191) Li, X.; Choy, W. C. H.; Huo, L.; Xie, F.; Sha, W. E. I.; Ding, B.; Guo, X.; Li, Y.; Hou, J.; You, J.; Yang, Y. *Dual Plasmonic Nanostructures for High Performance Inverted Organic Solar Cells*, *Adv. Mater.* **2012**, *24*, 3046-3052.

(192) Li, J. F.; Tian, Z. Q. *Shell-Isolated Nanoparticle-Enhanced Raman Spectroscopy (Shiners)*, *Frontiers of Surface-Enhanced Raman Scattering: Single Nanoparticles and Single Cells* **2014**, *464*, 163-192.

9. Author Biographies

Su-Wen Hsu is a postdoctoral research associate working with Prof. Andrea R. Tao in the Department of NanoEngineering at the University of California, San Diego. He received his Ph.D. from the University of California, San Diego in 2014 under the supervision of Prof. Andrea R. Tao. During his Ph.D., he studied the optical properties of semiconductor nanocrystals and their applications. His current research is mainly focused on the design of metal plasmonic nanojunctions by self-assembly and their applications.

Andrea L. Rodarte is a postdoctoral research associate working with Prof. Andrea R. Tao in the Department of NanoEngineering at the University of California, San Diego. She received her Ph.D. from the University of California, Merced in 2014 under the supervision of Prof. Linda S. Hirst and Prof. Sayantani Ghosh. During her Ph.D., she studied dispersions of semiconductor quantum dots in thermotropic liquid crystalline media. Her current research is focused on exploring plasmonic nanoparticles for biosensing and chemical sensing using surface-enhanced Raman spectroscopy.

Gaurav Arya is an Associate Professor in the Department of NanoEngineering at the University of California, San Diego (UCSD). He received his BTech in Chemical Engineering from the Indian Institute of Technology, Bombay in 1998, and PhD, also in Chemical Engineering, from the University of Notre Dame in 2003. He did his postdoctoral research at Princeton University and held an assistant research scientist position at New York University prior to joining UCSD. His research group uses advanced molecular simulation techniques to study a variety of nanoengineering and biophysical systems of interest, including polymer-nanoparticle composites, DNA nanotechnology, genome organization, and viral DNA packaging motors.

Madhura Som is a doctoral student in the Department of NanoEngineering at the University of California, San Diego (UCSD). She received her B.Tech. in Applied Electronics and Instrumentation Engineering from the Heritage Institute of Technology, West Bengal, India in 2011 and M.S. in Materials Science and Engineering from the State University of New York (SUNY) at Stony Brook in 2013. Her current research is on engineering nanoparticle-protein and nanoparticle-cell interactions using surface chemistry approaches for sensing, delivery and therapeutic applications.

Andrea R. Tao is an Associate Professor in the Department of NanoEngineering at the University of California, San Diego. She received her B.S. from Harvard University in Chemistry and Physics in 2002 working on mesoscale self-assembly, and her Ph.D. from UC Berkeley in Chemistry in 2007 on metal nanocrystal synthesis and assembly. She was a UC Office of the President Postdoctoral Fellow at UC Santa Barbara prior to joining UCSD, and studied the assembly of optical proteins in squid iridophores. Her research group develops new methods of organizing and manipulating nanoscale building blocks for the creation of next-generation, multifunctional nanocomposite materials.